Physical Oceanography in the Marshall Islands Area

Bikini and Nearby Atolls, Marshall Islands

GEOLOGICAL SURVEY PROFESSIONAL PAPER 260-R

Physical Oceanography in the Marshall Islands Area

By HAN-LEE MAO and KOZO YOSHIDA

Bikini and Nearby Atolls, Marshall Islands

GEOLOGICAL SURVEY PROFESSIONAL PAPER 260-R

UNITED STATES GOVERNMENT PRINTING OFFICE, WASHINGTON : 1955

UNITED STATES DEPARTMENT OF THE INTERIOR

Douglas McKay, *Secretary*

GEOLOGICAL SURVEY

W. E. Wrather, *Director*

For sale by the Superintendent of Documents, U. S. Government Printing Office
Washington 25, D. C. - Price 35 cents (paper cover)

CONTENTS

ILLUSTRATIONS

BIKINI AND NEARBY ATOLLS, MARSHALL ISLANDS

PHYSICAL OCEANOGRAPHY IN THE MARSHALL ISLANDS AREA[1]

By HAN-LEE MAO and KOZO YOSHIDA

ABSTRACT

The major features of physical oceanography in the Marshall Islands area are described in separate sections. Owing to the important role played by the system of water circulation in the shaping of other features, discussion of the circulation system is somewhat stressed. In addition to the flow patterns derived from dynamic anomalies, some directly measured current data are included, the large-size horizontal eddies which appear in the boundary zone between the North Equatorial Current and the Equatorial Countercurrent are discussed, and computations of mass transport are made. Distribution of temperature, salinity, density, and temperature-salinity (T–S) relationships are discussed mainly in light of the circulation system and the characteristics and movement of water masses. Only some general remarks are made on the distribution of oxygen because of the scarcity of data available.

An outstanding feature which appears to characterize physical oceanography in this area is the unique distribution of all the major properties in the areas of large eddies. It is to be noted that particular attention is always placed on the descriptions and interpretations of these outstanding features in this area of eddies.

INTRODUCTION

The primary purpose of this work is to present the general features of physical oceanography, except waves and tides, in the Marshall Islands area. The geographical area covered by this report extends from latitude 5° S. to 20° N. and from longitude 155° E. to 175° E. However, owing to the scarcity of data—especially, more recent data—south of the Equator, conclusions drawn as to the Southern Hemisphere are tentative.

General distribution of oceanographic conditions in this area is shown on horizontal and vertical charts. In this report only the major features are described, and reasonable explanations are given. Particular emphasis is always placed on the interrelated phenomena in various aspects.

The data which we used here are derived from (1) United States Operation Crossroads from 11 March to 10 August 1946 (fig. 179A) and (2) Japanese Hydrographic Investigations from 1933 to 1941 (fig. 179B). For convenience, we shall refer to these two sets of data as the Crossroads data and the Japanese data. The value of the Crossroads data, which were taken more recently and with more modern instruments, is offset by the limited number of stations occupied, particularly since most of the stations were concentrated around Bikini Atoll. Very few stations were occupied south of latitude 10° N., and therefore available information in the Equatorial Countercurrent area is far from sufficient. On the other hand, the Japanese data have merit because many stations (670) were used and because there was a rather even distribution of stations. These advantages are partly offset by the inhomogeneity of the data. This inhomogeneity may be real, in the sense that it represents the actual short- or long-period variations of the oceanic conditions during a period of almost 10 years. However, it may also be due partly to progress in the use of instruments and the consequent accuracy of observation in oceanographic investigation.

In view of this, the two sets of data are charted separately, and only major features which appeared in them are discussed. To reveal some characteristics of the seasonal variations in hydrographic conditions, the Japanese data were divided, wherever possible, into two seasons: summer, from April to September, and winter, from October to March. This division is mainly in accord with the study by Robinson (1954) of bathythermograph temperatures in the same area. However, it must be remarked that the monthly distribution of data is very uneven.

It is unfortunate that, owing to the lack of reliable data on wind and humidity covering a sufficiently long period, the energy budget, one of the most interesting topics in physical oceanography, cannot be pursued in this study.

[1] Contribution from the Scripps Institution of Oceanography, New Series, No. 644.

NOTE.—This work is partly supported by the Office of Naval Research.

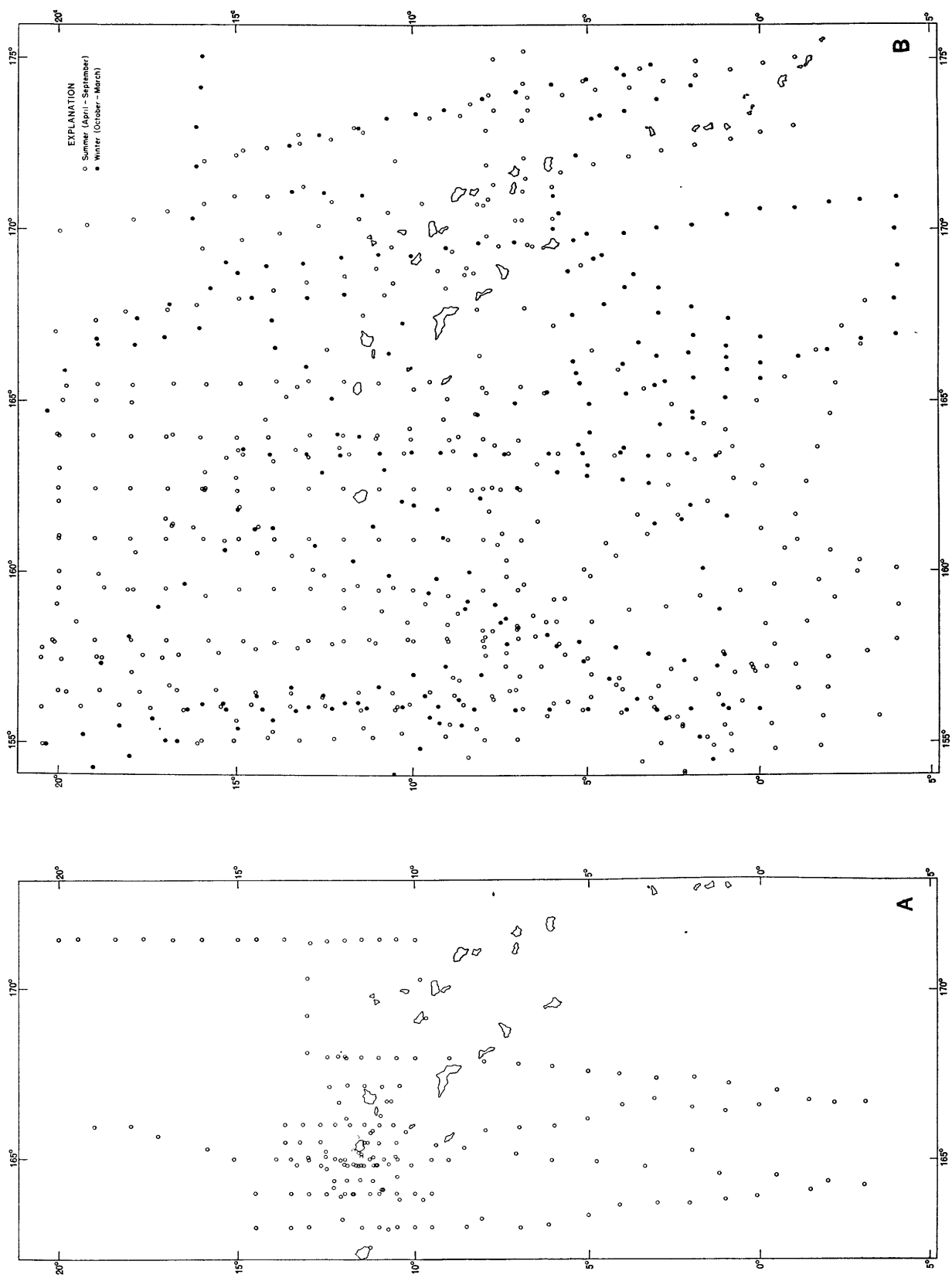

FIGURE 179.—Station plans. *A*, U. S. Operation Crossroads, March 11 to August 10, 1946. *B*, Japanese Hydrographic Investigations, 1933–41.

ACKNOWLEDGMENT

The authors wish to express their sincere thanks to Prof. C. E. Palmer, Institute of Geophysics, University of California at Los Angeles, who kindly furnished some unpublished original wind data; and to Mr. Daitaro Shoji, Japanese Hydrographic Office, who supplied valuable suggestions for analyzing Japanese data. The permission to use and publish the Japanese hydrographic data was kindly granted by Dr. Kanji Suda, Director of the Japanese Hydrographic Office.

WATER CIRCULATION

Apart from water circulation in the upper mixed layer, which has been separately discussed in another study by the writers and Paul L. Horrer (Yoshida others, 1953), the water circulation in this investigation is that delineated by geostrophic flow only. Some direct current measurements from the Japanese Hydrographic Office (Japanese Hydrographic Department, 1933; Japanese Hydrographic Bureau, 1948; and Japanese Maritime Safety Agency, 1950) are included for comparison. In the dynamic computations a depth of 1,000 m is customarily adopted as the level of no motion.

For brevity, the major features of geostrophic circulation in the Marshall Islands area are presented in four parts. First, the presentation of vertical profiles of latitudinal variations of isobaric topography is intended to give a brief view of current systems. Second, the general flow pattern at various levels is illustrated by charts of horizontal currents. Third, dynamics of large-scale, semipermanent horizontal eddies, which appear outstandingly in the boundary between the Countercurrent system and the North Equatorial Current system, call for closer attention and are discussed separately. Fourth, mass transport from the surface to the depth of no motion is calculated.

LATITUDINAL VARIATION OF ISOBARIC TOPOGRAPHIES

Three sections of vertical profile of isobaric topography at equigeopotential surfaces, representing, respectively, the Crossroads data, the Japanese data for summer, and the Japanese data for winter are shown as figures 180. These sections are selected in such a way that each passes through approximately the central part of the area and trends approximately northward. In order to include a maximum number of stations in each section, those stations which do not fall along the north-trending line exactly, but within the distance of ½° of longitude, are also included in the vertical profile. Thus, we have selected lines running approximately along lontitude 166° E. and 164° E for the Crossroads and the Japanese sections, respectively.

Some of the most pronounced features from these sections of vertical profiles are summarized as follows:

At the Equator and in its vicinity the isobaric topography of the Crossroads and the Japanese sections present opposite features. In the Crossroads section (fig. 180*A*), all isobaric surfaces reach maximum values; in the Japanese sections (fig. 180B, C) all isobaric surfaces attain minimum values. Figure 180*A* indicates that for the Crossroads sections the current flows toward the East near the Equator in both hemispheres; that is to say, the Countercurrent system extends to the Southern Hemisphere, whereas figure 180*B*, *C* shows the South Equatorial Current system extending to a latitude of about 2°–3° N. Although it is generally recognized that the Countercurrent system is always found in the Northern Hemisphere, the extension of the system into the Southern Hemisphere is, of course, dynamically possible. Dynamic conditions require only that all isobaric surfaces must reach their extreme values at the Equator or near it, regardless of whether the value is a maximum or a minimum. In fact, Sverdrup (Sverdrup and Fleming, 1944) noted in the Western Pacific that the Carnegie results showed the Countercurrent extending from latitude 6°20′ N. to 3°20′ S. This northern limit coincides very well with our figure 180*A*; the southern limit of the Countercurrent is not clear in the Crossroads sections. The temporal and spatial variations of the position of the Countercurrent have been mentioned in Robinson's recent work in the analysis of bathythermograph data of the same area (Robinson, 1954). It is unfortunate that owing to the heterogeneity of the Japanese data no definite conclusion can be drawn as to the nature of seasonal variations of the current systems at or near the Equator.

From the southern boundary of the Countercurrent system, isobaric surfaces in all three sections dip to the north, and reach their minimal values—that is, the northern boundary of the Countercurrent system, at latitudes about 6° N. and 9° N. respectively for the Crossroads and the Japanese sections. Comparing figure 180*A* and figure 180*B*, *C*, it is immediately seen that the positions of current systems from the Crossroads sections shift about 3° of latitude southward from those of the Japanese sections. Positions of three Equatorial current systems of the Japanese sections agree fairly well with others. The nature of the "southerly shift" of the Crossroads sections requires further investigation, and it will be discussed in the section on mass transport.

Commencing at the northern boundary of the Countercurrent, we enter into the system of the Northern Equatorial Current; in figure 180*A*, *B*, *C*, all

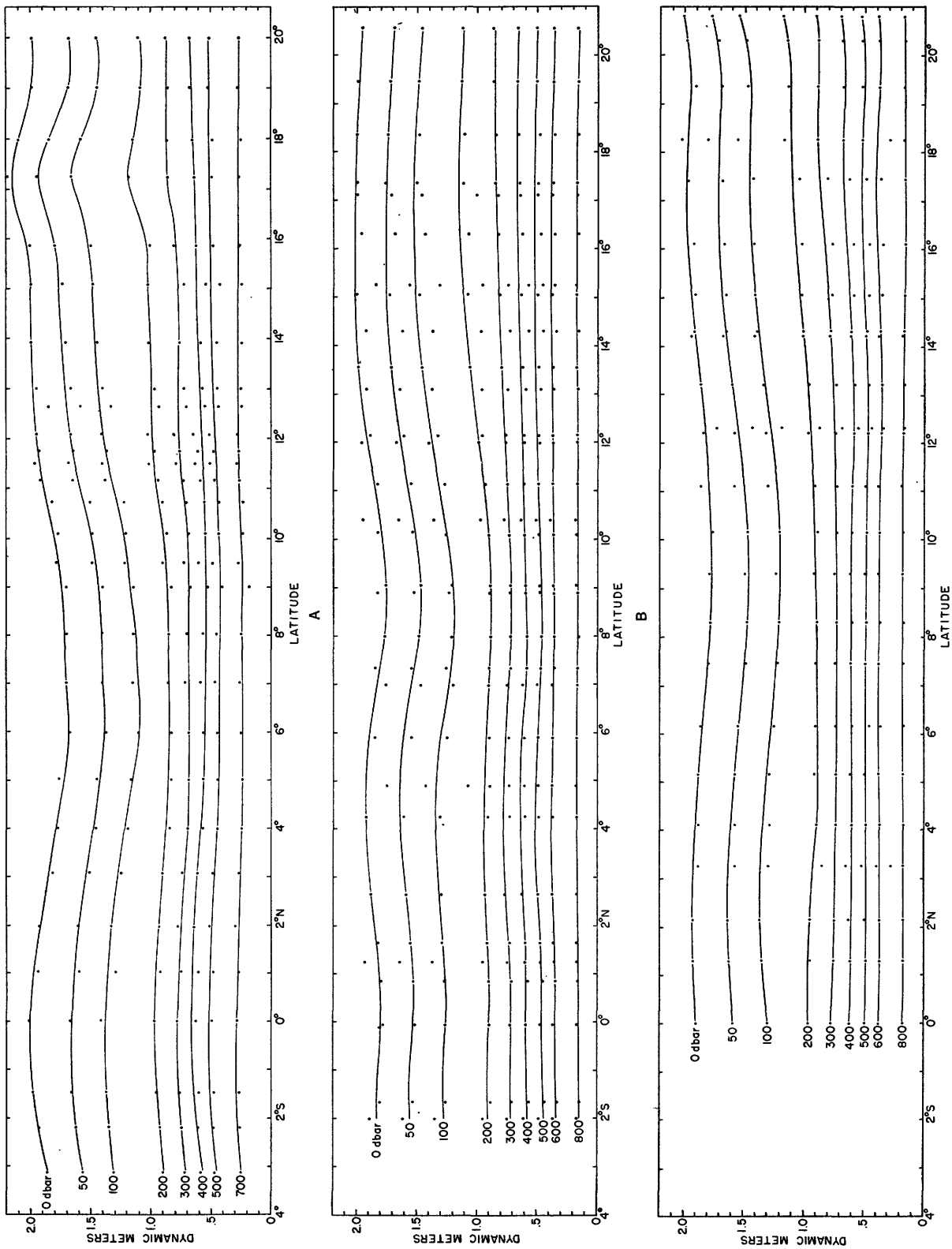

FIGURE 180.—Vertical distribution of isobaric topography relative to the 1,000-dbar surface. *A*, From Crossroads data, March to August 1946. *B*, From Japanese data, 1933–41, summer season. *C*, From Japanese data, 1933–41, winter season.

isobaric surfaces north of the boundary tilt up toward the north, meaning that the currents flow due west. The northern boundary of the Northern Equatorial Current system is probably out of the area considered in this study.

Another unusual feature in the Crossroads section is the appearance between latitudes 16°–18° N. of a relatively sharp "hump" in the isobaric topography in figure 180*A*, meaning that a narrow band of strong easterly current exists there. Owing to the scarcity of observations there and the fact that no similar phenomenon occurs in the Japanese sections or other data, it is questionable whether this "hump" does mean a true easterly current. It should, however, be mentioned that a similar "hump" had been noted by Cromwell (1950)—at similar latitudes (18°–20° N.), though at a very different longitude (approximately along longitude 158° W.)—in one section of the isobaric topography in his study of the oceanography of the Mid-Pacific.

HORIZONTAL CURRENT SYSTEMS AT VARIOUS DEPTHS

Three levels—that is, at the surface and at 250 m and 500 m—have been chosen as representative of surface (and near surface), middepth, and deeper layers. Since there shall be no discussion of the current features which do not appear in the charts of geostrophic flow, readers who are especially interested in the characteristics of surface flow in this area are referred to another paper (Yoshida and others, 1953).

CURRENT AT SURFACE OR NEAR SURFACE

[Fig. 181]

One of the most important features which appears in all these figures is the cyclonic eddy (or several eddies) at the northern boundary of the Countercurrent system. Its location is about latitude 6°–8° N. in the Crossroads data (fig. 181*A*) and latitude 8°–10° N. in the Japanese data (figs. 181*B*, *C*). Because of the outstanding nature of these eddies and their important bearing on the other aspects of physical oceanography, they will be discussed in detail immediately following this section.

At the surface, velocity of the Countercurrent is fairly high, though it varies considerably within the system. The highest velocity, about 2 knots, generally appears at the southern edge of the eddies; that is, at about latitude 2°–4° N. in figure 181*A* and at latitude 4°–6° N. in figure 181*B*, *C*. Since the validity of the geostrophic flow at very low latitudes is open to question, too much emphasis should not be placed on the numerical values of current velocity calculated from dynamic computations.

The over-all mean of current velocity, from dynamic computation of the North Equatorial Current system in this region, is about ⅓ knot. The highest velocity reaches 1 knot in some localities at the northern edge of the eddies, at about latitude 10°–12° N. and latitude 12°–14° N. for the Crossroads and the Japanese results, respectively. The "looping" of the current in the northern side of Bikini Atoll is probably due to the damping effect of the island on the flow.

The narrow band of the (uncertain) easterly flow which appears at latitude 16°–18° N. from the Crossroads results was presented in the chart only tentatively. The velocity of this flow is relatively high, amounting to about 0.8 to 1.0 knot.

CURRENT AT MIDDEPTH LEVELS

[Fig. 182]

The characteristic features of the geostrophic flow patterns at middepths are quite similar to those at the upper levels. The intensity of the horizontal eddies at the northern boundary of the Countercurrent becomes very weak at these levels, as shown in figure 182*A*, *B*, but remains practically unchanged in figure 182*C*. The size of these eddies seems to increase with depth, and a large part of the territory of the Countercurrent at upper levels is occupied by horizontal eddies at middepth. This agrees with Sverdrup's suggestion that the Equatorial Countercurrent is the flow of a relatively thin layer. However, it does not necessarily mean that the Southern Equatorial Current system underlies the Countercurrent system as Cromwell (1950) remarked. In fact, both theoretical results (Yoshida and others, 1953) and direct measurements [2] have shown that the opposite might be true. A reasonable interpretation might be that the Countercurrent velocities decrease very suddenly below the intersurface of discontinuity or the thermocline. This renders the velocities of flow there almost immeasurable, a fact noted by the Shellback Expedition and conforming to figure 182*A*, *B*.

CURRENTS AT DEEPER LAYERS

[Fig. 183]

Except for the continuing decrease of velocities, the geostrophic flow pattern at a depth of 500 m retains characteristics quite similar to those of upper levels. The horizontal eddies at this depth now become so large that the whole system of the Countercurrent is nearly merged into the eddies, but the direction is still due east. As depth increases the damping effect of the islands on the eddies becomes more pronounced, because (1) the cross-sectional areas of the islands

[2] Wooster, W. S., 1952, Preliminary report, Shellback Expedition, May 17 to August 28, 1952, Univ. Calif. Scripps Inst. Oceanography, SIO Ref. 52-47 (mimeographed).

315915—55——2

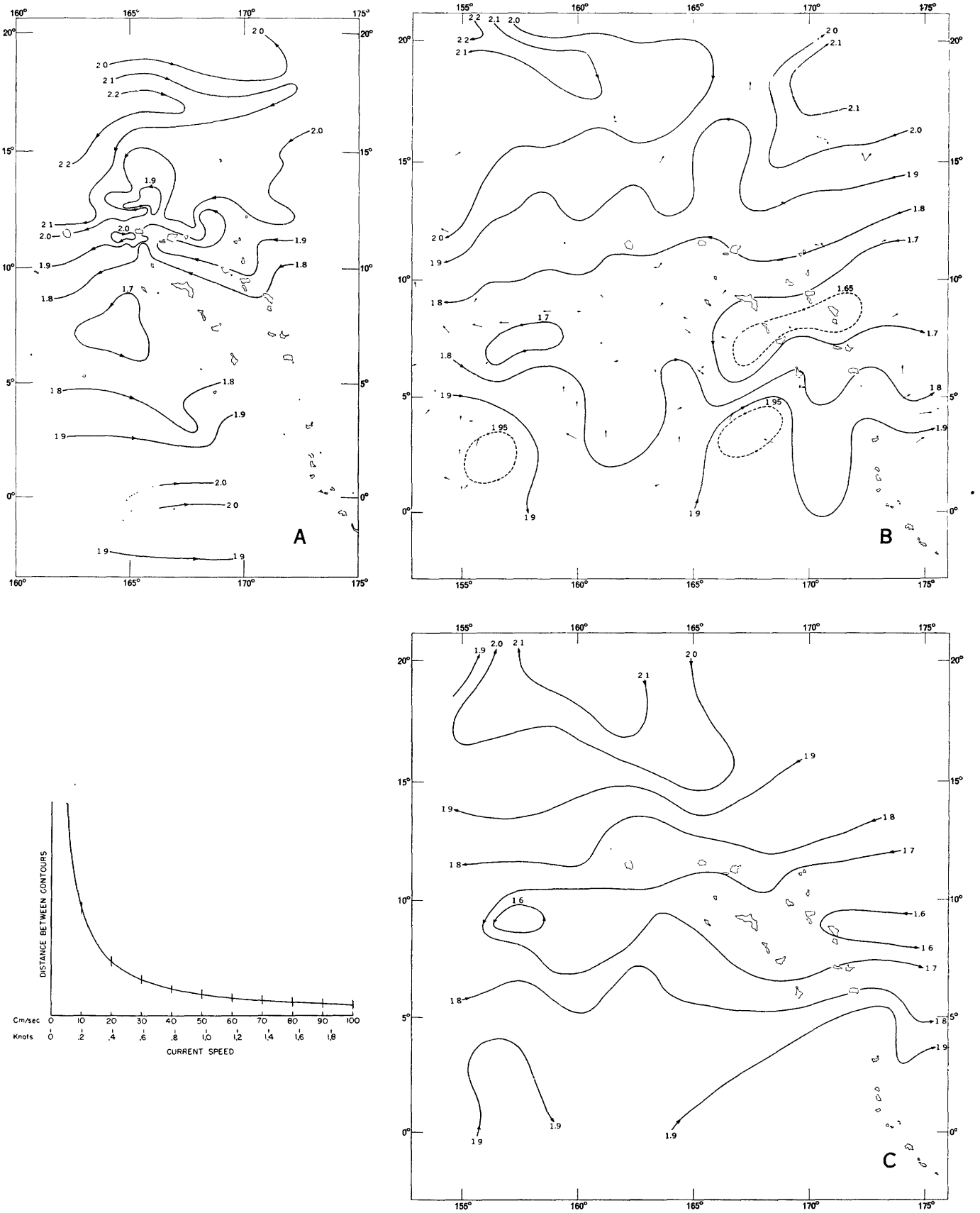

FIGURE 181.—Horizontal distribution of Dynamic-height anomalies at Surface. *A*, From Crossroads data, March to August 1946. *B*, From Japanese data, 1933–41, summer season. *C*, From Japanese data, 1933–41, winter season.

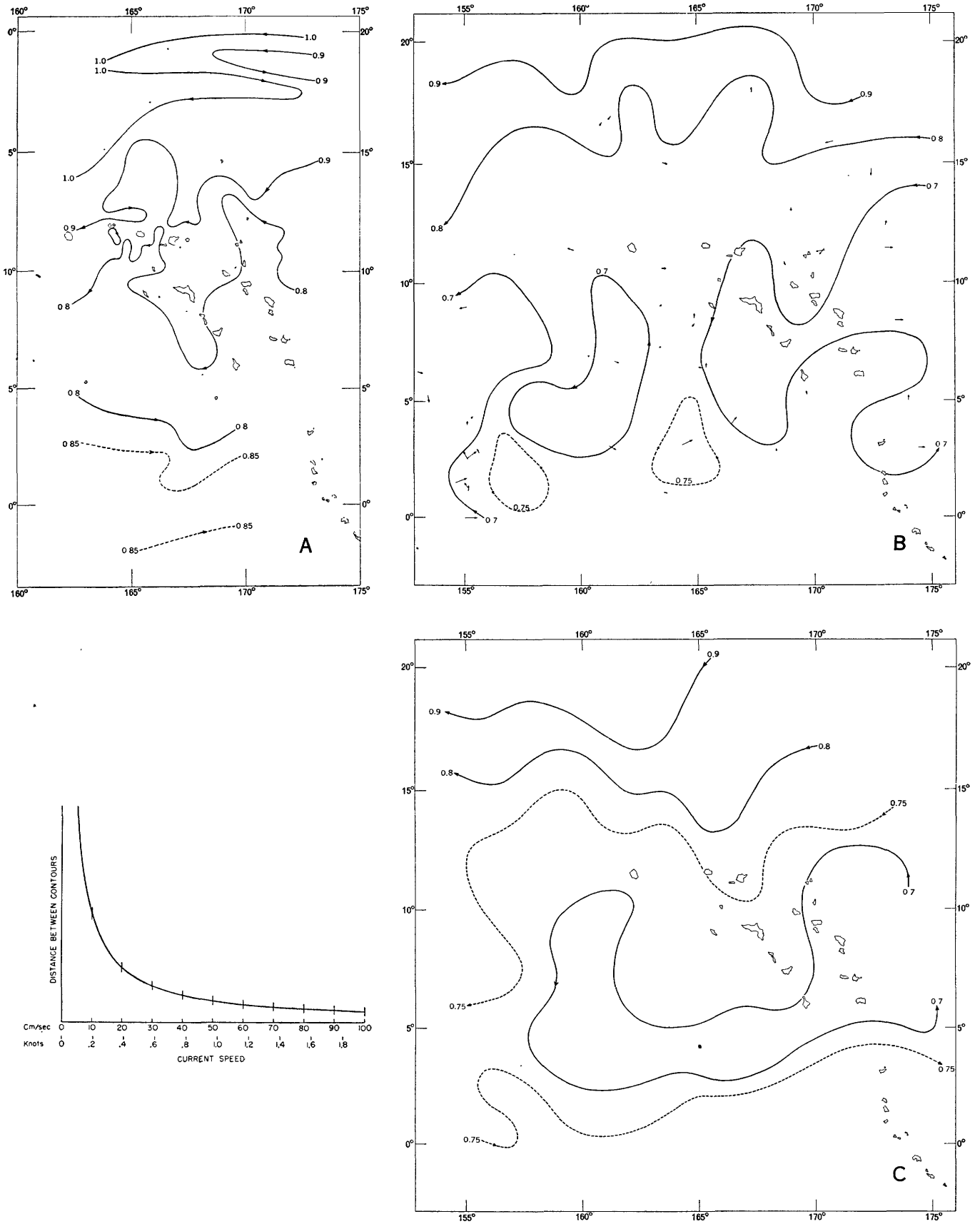

FIGURE 182.—Horizontal distribution of dynamic-height anomalies. *A*, At 250 meters, from Crossroads data, March to August 1946. *B*, At 300 meters, from Japanese data, 1933–41, summer season. *C*, At 300 meters, from Japanese data, 1933–41, winter season.

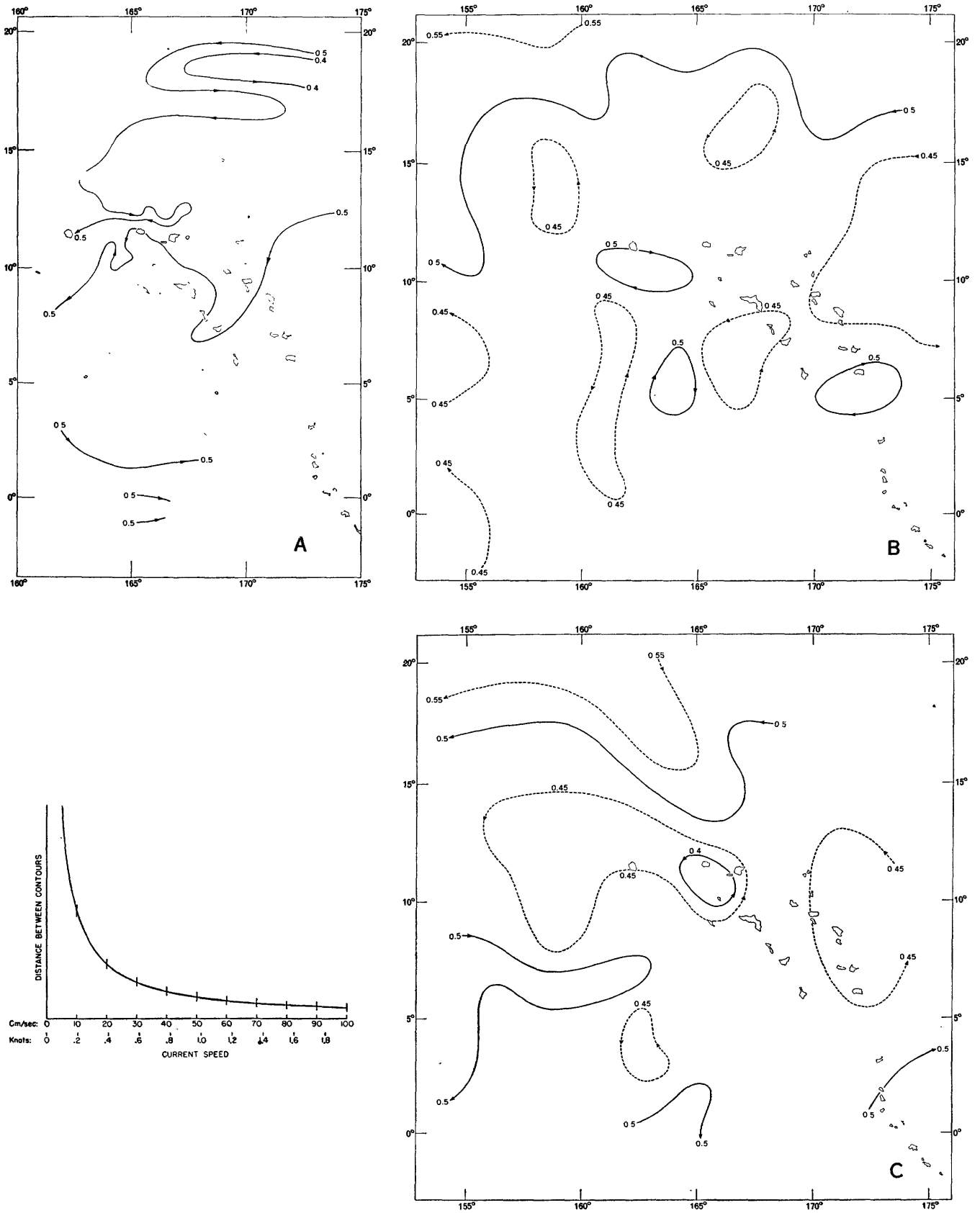

FIGURE 183.—Horizontal distribution of dynamic-height anomalies at 500 meters. *A*, From Crossroads data, March to August 1946. *B*, From Japanese data, 1933–41, summer season. *C*, From Japanese data, 1933–41, winter season.

increase with increasing depth, and (2) the eddies become so weak, and hence unstable, that they are very easy to split. It is clearly seen from figure 183*C* that the eddies are split into smaller ones.

It is also interesting to note that the narrow band of easterly flow at latitude 16°–18° N. in figure 183*A* maintains an unusually high velocity at such depth. This suggests it may be apparent, owing to tidal effect, rather than a reality.

COMPARISON OF GEOSTROPHIC FLOW AND DIRECT MEASUREMENT OF CURRENT

During those years when the Japanese Hydrographic Office was surveying this area, certain direct measurements of current were taken by two methods: by use of the floating buoy and by use of the Ekman current meter, which was lowered to a preassigned level from an anchored or drifting ship. When the floating ship is on the open sea, to determine the drift of the ship to an acceptable degree of accuracy is not easy. The method which the Japanese Hydrographic Office (1933) adopted is to assume a level of no motion, thus allowing the drift of the ship and consequently the measured "relative current" with reference to the fixed level of no motion to be determined. For the area of the tropical Pacific, a depth of 400 m was accepted as the level of no motion.

It is to be noted that the accuracy of the results of direct measurement of current is affected by (1) the instrumental accuracy, (2) effect of the tidal current, and (3) temporal and local variations, especially in the upper wind-stirred layer. The Japanese Hydrographic Office (1933) stated that in general they believed the accuracy of their current meters was within 10 degrees in direction and 0.2 knot (10 cm/sec) in magnitude. For the whole area of concern the maximum magnitude of tidal current was calculated about 5 cm/sec, if we assume that the mean depth is 2,000 m and that the maximum amplitude of the tides in the open sea is 50 cm. Thus, the probable error due to instrumental and tidal effects amounts to 15 cm/sec, not including such temporal variations as wind effect.

It is immediately seen that when the currents are weak, the results of the direct measurement of currents are not very reliable because the actual magnitude of current velocity might be smaller than the probable error. However, comparing the results of the direct measurements—which for the purpose of convenience are entered as arrows in the horizontal current charts at the surface and at 300 m, shown as figures 181*B* and 182*B*—with geostrophic flow at corresponding depth, the agreement of their major features is fairly satisfactory. Some of them can be stated as follows:

In moderate and strong current, the direct measurements provide sufficient and reliable information of the magnitude as well as direction of the current velocities.

The positions of the Equatorial Current systems, derived from geostrophic flow and direct measurement, generally agree with each other.

The results of direct measurement appear to indicate the existence of eddies at the northern boundary of the Countercurrent, where the arrows of measured current seem to have a counterclockwise rotation.

DYNAMICS OF LARGE HORIZONTAL EDDIES

GENERATION

The charts of dynamic topography appear to indicate that there exist large-scale horizontal eddies between 4° N. and 10° N., corresponding to the northern boundary of the Countercurrent. Although it is not necessarily evident whether the occurrence of these eddies is real or apparent, some of the recent results from direct measurements of currents appear to support the existence of these eddies (Cromwell, 1950).[3]

It is to be remarked that each of the eddies found in our data has an approximate radius of several hundred kilometers and that no eddy is found in the southern boundary of the Countercurrent.

Although the cause of these eddies is not yet clear, several possible interpretations are proposed, as follows:

First, it is considered very probable that these eddies are of a similar nature to those found in the outer area of the Gulf Stream. The system which involves the Countercurrent flowing in the opposite direction to the surrounding currents may be analogous to the Gulf Stream system. The eddies are expected to be generated by cut-off from the meandering current system; this can be produced in the boundary zone between two different current systems and actually is found to exist. (Haurwitz and Panofsky, 1950.)

It is desirable to examine the question of whether this consideration can account for the wavelength of the meandering or the dimension of the eddy and also for the fact that no eddy can be found in the southern boundary of the Countercurrent. A theoretical investigation will be made in the near future. In the present report our discussion is confined to possibilities.

The second possibility is related to turbulence in this boundary zone between two different systems. Since in such an area the current shear is very large, we can expect considerable intensive horizontal mixing, and under this circumstance some external disturbances can produce eddies in this region (fig. 184). Such disturbances may be caused by bottom topography, islands, or steady or unsteady meteorological conditions. So far as we have examined, the predominance of the effects

[3] Also Wooster, W. S., op cit.

of islands is considered most probable, judging from the location of the eddies. Furthermore, the existence of islands may effect the flow in such a manner that the intensity of turbulence increases owing to friction. Since most of the islands in this area are located from 5° N. to 12° N. and from 165° E. to 173° E. this consideration might lead to an interpretation of the particular localities and dimensions of the eddies.

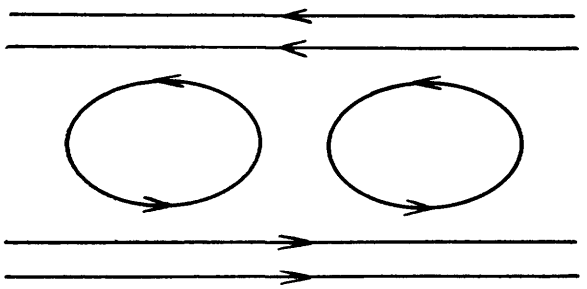

FIGURE 184.—A schematic representation of horizontal eddies produced in the boundary shear zone.

The barrier effect of islands may be interpreted in another way, which provides the third possibility: the islands which constitute the Ratak Chain and Ralik Chain are assumed to be some kind of barrier. Even where there is no significant turbulent motion or meandering it may be possible to expect the eddies, as illustrated in figure 185.

Which of these possibilities is predominant is not easy to say. Actually, it is most probable that these factors act together, and in this connection it is desirable that further observations and theoretical considerations be made.

In the theoretical study of the equatorial currents in the upper mixed layer by the present writers and Paul L. Horrer (Yoshida and others, 1953), effects of lateral mixing were discussed. Some considerations of lateral mixing in connection with the dynamics of eddies will be presented later.

MAINTENANCE

It is seen that the counterclockwise circulation associates two forces, both of which are directed outward: Coriolis and centrifugal. To maintain a steady state, radial pressure gradient is required to be directed inward. In the northern boundary of the Countercurrent this condition is actually fulfilled (fig. 186*A*). On the other hand, the major pressure field near the southern boundary of the Countercurrent appears to indicate that no clockwise eddy can be established (fig. 186*B*). The minimum of integrated pressure P is found at about 6° N., from the Crossroads data, and at about 8° to 10° N., from the Japanese data, and these minima coincide with the centers of the boundary zones or horizontal eddies.

It may thus be suggested that lateral mixing takes place at the southern boundary of the Countercurrent and that momentum is exchanged by small, variable, irregular eddies between two current systems. On the other hand, in the northern boundary zone the effect of mixing is considered a little differently. First, owing

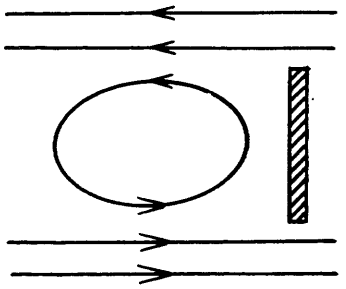

FIGURE 185.—A schematic representation of horizontal eddy caused by a barrier.

to the effects of the islands as well as the large current shear associated with the major current field, the turbulence may be more intensive, and small, irregular eddies are easily generated. Thus, to establish a steady-state distribution of current, lateral mixing may

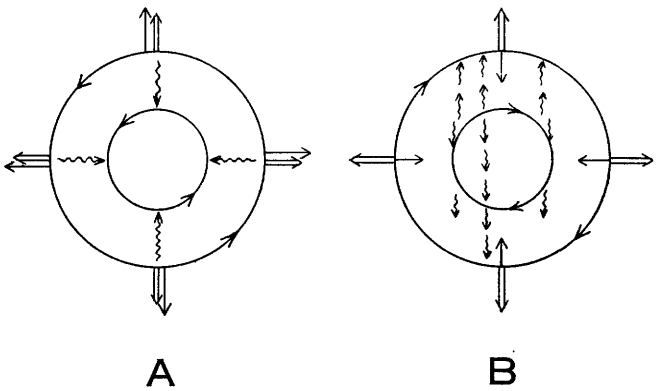

FIGURE 186.—A schematical representation of forces acting in a horizontal eddy. A, Northern boundary of Equatorial Countercurrent. B, Southern boundary of Equatorial Countercurrent. Explanation of symbols: Single straight arrow represents a Coriolis-force vector; double straight arrow represents a centrifugal-force vector; wavy single arrow represents a pressure-gradient-force vector.

play an important role. This current field in the large eddy should also associate the corresponding radial pressure gradient. Since the velocity field as well as the pressure gradient field is not completely free from those in the surrounding systems it may be expected that such forces as Coriolis, centrifugal, pressure-gradient, and horizontal mixing are acting simultaneously and tending to bring the field towards a steady state. Vertical mixing might also play a part in such adjustments, but it is supposedly less significant. If this stationary state is established, mixing effects will become less. Any temporary or local deviation from the stable configuration can be cancelled owing to these

mutual arrangements. Thus, in this region horizontal mixing contributes to maintaining the boundary eddies instead of causing direct exchange of momentum between the two major current systems.

MASS TRANSPORT

The advancement of mass-transport theories by Sverdrup (1947), Reid (1948a), Munk (1950) and many others marks an important step towards our understanding of water circulation in the oceans. Reid's result of mass transport, based on the statistical mean values of wind stress, provides us with a general feature for the Equatorial Eastern Pacific. It is interesting to see whether Reid's major features also apply for the Marshall Islands area. Furthermore, in the previous sections we mentioned that the current systems obtained from dynamic computations of the Crossroads data are apparently shifting about 3° of latitude southward in comparison with those obtained from the Japanese data. Does the same phenomenon also appear in the picture of mass transport? If so, what is the possible nature of such a shift? The intent is to investigate these questions in this section.

In order to compute the mass transport for a specific region such as the one considered in this study, trustworthy local wind data covering a sufficiently long period are required. It is unfortunate that the wind data from Operation Crossroads did not cover a period long enough so that we can have sufficient confidence to use them to compute the mass transport of a steady flow. The wind data from Japanese cruises are apparently too low, because of the old-type wind vane then used.

Under these circumstances, to compute the mass transport of this area it seems desirable to supplement the wind data from Operation Crossroads with data from Operation Greenhouse, which was kindly put at our disposal by Dr. C. E. Palmer,[4] Institute of Geophysics, University of California at Los Angeles. This combination is, of course, a sheer necessity from the statistical point of view. It is to be noted that the major features of these two sets of data are so similar that the combination is considered justifiable. The table below shows the number of wind observations of the two operations.

Stations	Latitude	Longitude	Number of wind observations—		
			Operation Cross-roads	Operation Green-house	Total
Wake	19°18′ N.	166°37′ E.	232	273	505
Bikini			151	0	151
Eniwetok	11°21′ N.	162°31′ E.	232	335	567
Kwajalein	8°43′ N.	167°44′ E.	230	333	563
Truk	7°15′ N.	151°51′ E.	0	224	224
Majuro	7°06′ N.	171°24′ E.	195	281	476
Ponape	6°50′ N.	158°12′ E.	0	233	233
Kusaie	5°20′ N.	163°05′ E.	0	275	275
Bikati	3°02′ N.	172°50′ E.	0	281	281
Tarawa	1°21′ N.	172°56′ E.	221	0	221
Narau	0°33′ S.	166°55′ E.	0	272	272

[4] Palmer, C. E., 1951, The tropical Pacific project. Thirteenth Report: Institute of Geophysics, Univ. Calif. Los Angeles (mimeographed).

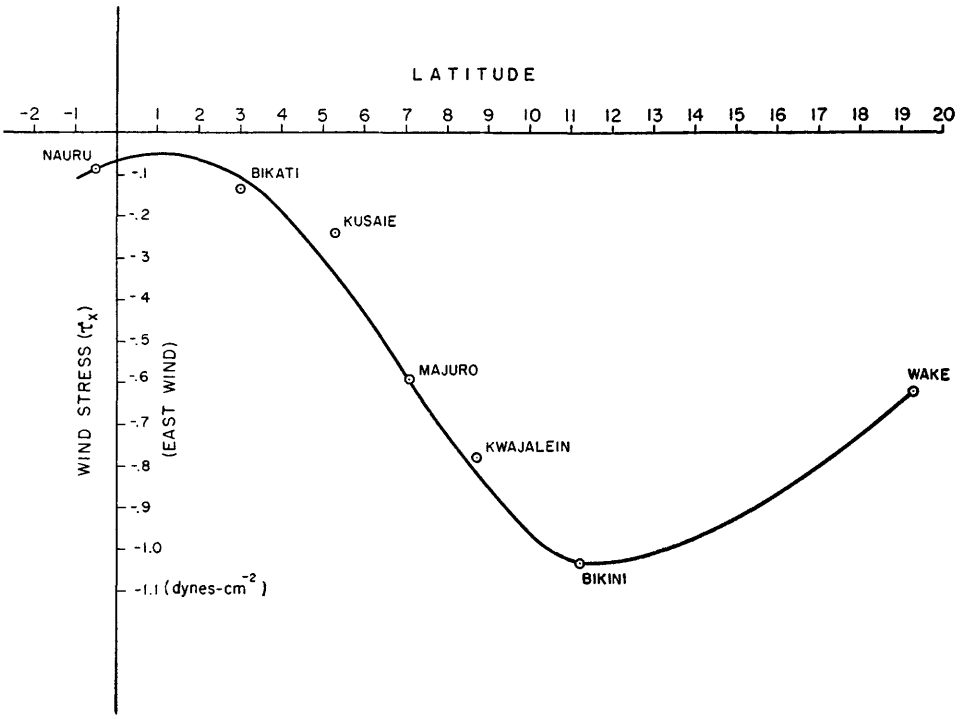

FIGURE 187.—Latitude dependence of mean wind stress (τ_x), from Crossroads data, March to August 1946, and from Greenhouse data.

In the computations of wind stress, Reid's method has been adopted. A smooth curve of best fit for the latitudinal variation was drawn from the computational results. Owing to the relatively small extension of the area east and west, only variations north and south are concerned. For those stations within 1° of latitude, such as Bikini and Eniwetok Atolls, Truk, Majuro, and Ponape, the mean value was taken by averaging the number of stations considered.

The computational results show that for most of the stations the north-trending component of the wind stress is normal to the zero mean, or nearly so. Therefore only the east-trending component should be considered. The latitudinal dependence of the east-trending component of the mean stress τ_x, taken from the wind data of Operation Crossroads and Operation Greenhouse, is shown in figure 187.

Values of the first and the second derivatives of τ_x with respect to latitudinal distance—that is, $\delta\tau_x/\delta y$ and $\delta^2\tau_x/\delta y^2$—are the finite differences taken from the curve in figure 187. The vertically integrated pressure P is evaluated from the numerical integration of the expression

$$P=\int_0^d p\,dz,$$

where p is the hydrostatic pressure and integration is performed from the sea surface to the depth of no motion, assumed a level of 1,000 m. The horizontal gradient of P north and south—that is $\delta P/\delta y$ from the Crossroads data along a section running approximately along 166° E. (shown in figure 180*A*) is calculated and entered in figure 188.

Reid shows that mass transport can be computed by two independent sets of solutions: one in terms of wind stress—for which Reid's solutions have been used—and the other based mainly on oceanographic data—for these data except for the region in the vicinity of the Equator, our solutions, as developed in another paper (Yoshida and others 1953), are essentially the same as those of Reid's. This is especially true when the wind component trends predominantly east and west and the horizontal gradient of P east and west is smaller than that north and south. Numerical computations by means of the second set of solutions show that the contributions of "drift current" to the mass transport is negligibly small. In other words, for practical purposes the second set of solutions is only an integration of geostrophic flow. Therefore, in the region of very low latitude only the first set of solutions (those in terms of wind stress) should be used. In the calculation of M_x by means of this set of solutions the quantity $|X_1-X_0|$ (the longitudinal distance between the eastern boundary and the western path) is assumed as 8×10^8 cm, that is, the approximate distance between the outer boundary of the California Current and the mean path of the area considered. Because of the small coverage of the area east and west, no reliable mean value of $\delta P/\delta x$ can be evaluated; therefore, in the calculations of $\overline{M}_y$, only the solution in terms of wind stress has been employed. The numerical results of longitudinal mass transport M_x as well as latitudinal mass transport $\overline{M}_y$ are entered in figures 189 and 190.

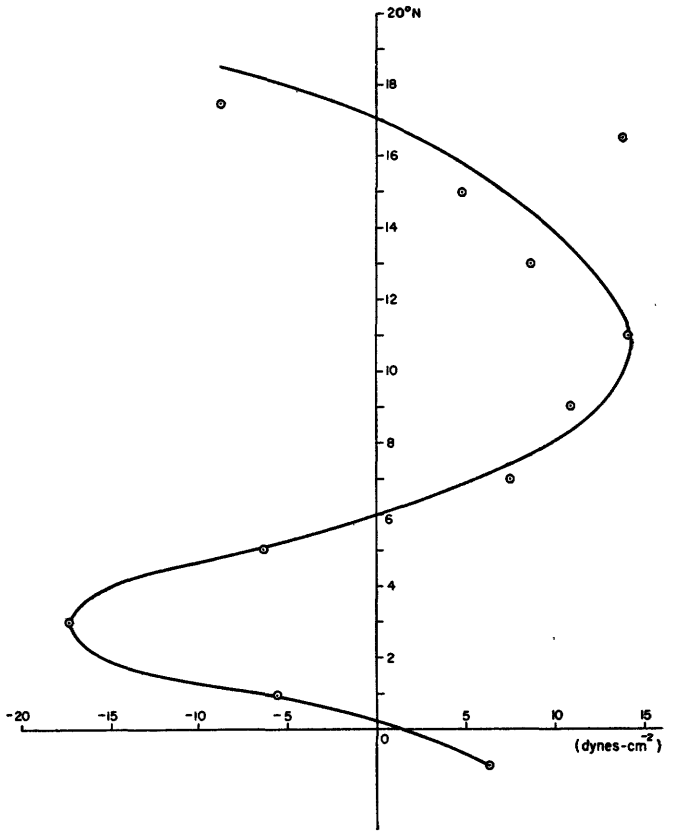

FIGURE 188.—Latitude dependence of integrated pressure gradient ($\delta P/\delta y$), from Crossroads data, March to August 1946.

The agreement of the results of M_x from two independent sets of solutions above latitude 6° N. in figure 189 is considered fairly satisfactory. This suggests that the wind data obtained from Operation Crossroads and Operation Greenhouse are able to account for the current systems shown by the oceanographic results of Operation Crossroads. Comparing our results of mass transport with Reid's, the southwardly shift is obvious. To determine whether this shift is semipermanent in this area demands additional wind observations.

DISTRIBUTION OF TEMPERATURE AND SALINITY

Values of temperature entering into this discussion were taken only from reversing-thermometer tempera-

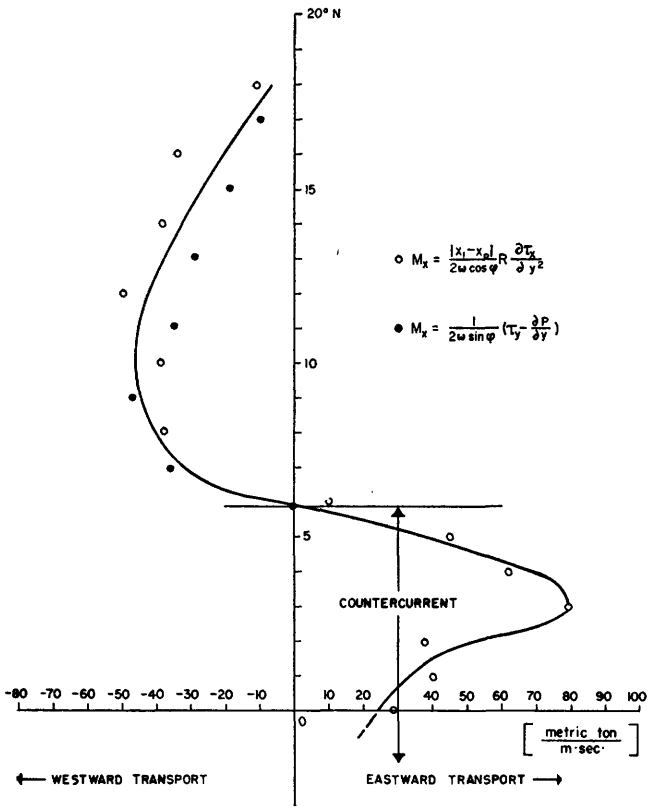

FIGURE 189.—Latitude dependence of east-west component of mass transport (M_x).

tures of the Crossroads data and the Japanese data. A separate study of bathythermograph temperatures for the upper 400 ft has already been made by Robinson (1954). Since a much larger number of bathythermograph temperatures than reversing-thermometer temperatures were available in the Marshall Islands area and furthermore, since the bathythermograph data were comparatively recently taken, their reliability is expected to be higher than some of the reversing-thermometer data, which were taken almost 20 years ago. Therefore, the reader who is especially interested in the detailed temperature distribution and its seasonal variations within the upper 400 ft should refer to Robinson's work.

VERTICAL DISTRIBUTION

To present a typical example, the vertical distribution of temperature and salinity (and its computed σ_t value) of Station B–39 (12°00′ N., 168°01′ E.; data taken on 12 July 1946) of the Crossroads results is shown in figure 191.

In the temperature profile, it is readily seen that the curve can be unmistakably divided into three parts: the topmost isothermal layer, the thermocline layer, and the layer of weak gradient. The topmost isothermal layer is also referred to as the homogeneous layer (Ekman), Zone of Agitation (Störungs Zone, Defant), convection layer (Sverdrup), upper mixed layer (Munk), wind-stirred layer (Munk) and others. These various names suggest that the uniformity of temperature within this topmost layer is mainly caused by (1) thorough mixing of water in this layer by ceaseless and vigorous mechanical stirring or agitation, and (2) by thermohaline convection near the surface.

In the salinity profile, the division of the curve into the topmost layer, the upper layer (characterized by salinity maximum), the intermediate layer (characterized by salinity minimum), and the deeper layer (characterized by weak-salinity gradient) is distinct.

The mirror image of the σ_t profile to that of temperature profile actually tells nothing more than the well-known fact that the density of sea water is, in general, predominantly determined by the water temperature and that it reflects it.

Figure 192 is given to present the characteristic features of latitude dependence of temperature at various depths. It should be noted that the longitudinal positions of these sections are the same as those of isobaric topographies—that is, for the Crossroads section (fig. 192*A*) the line running approximately along 164° E. and for the Japanese sections (fig. 192*B*, *C*) the line running along approximately 166° E.

To avoid the overcrowding of isotherms in the upper

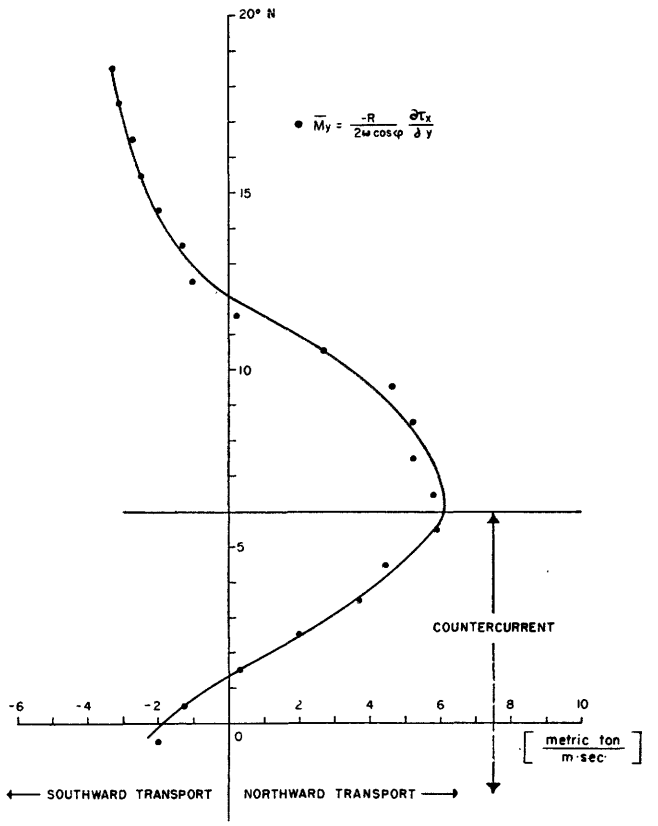

FIGURE 190.—Latitude dependence of north-south component of mass transport ($\overline{M}_y$).

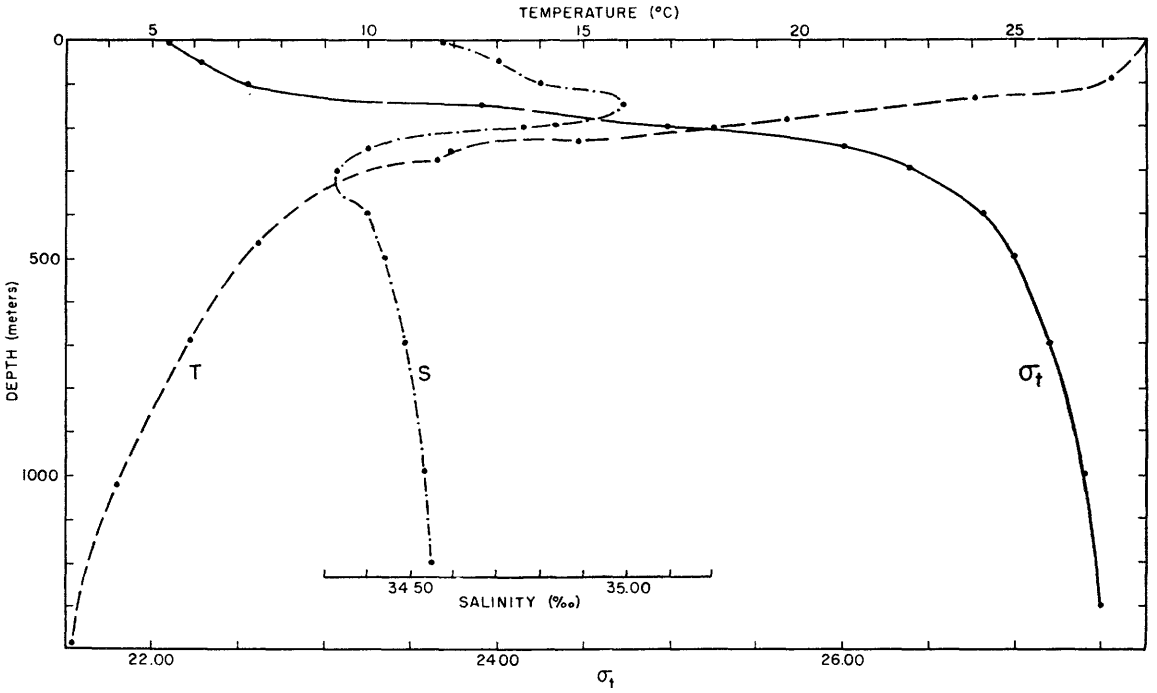

FIGURE 191.—Vertical distribution of temperature, salinity, and σ_t values at station B-39 (12°00′ N., 168°01′ E.), from Crossroads data, July 12, 1946.

layer, unequal isotherm intervals have to be chosen and depths of thermocline have to be omitted. However, in this area the substitution of the 28° C isotherm for the thermocline is satisfactory, at least for the low latitudes (lower than 10°–12° N.). Original temperature profiles show that for this region the thermocline is almost invariably at 28° C. For latitudes higher than 12° N. the thermocline is less distinctive, although as an average the 26° C isotherm is a good approximation.

Bearing these facts in mind, it is obvious from these figures that the thickness of the isothermal layer in this region generally lies between 50 m and 100 m, with an average thickness of about 75 m. Figure 192*B*, *C*, reveals that the isothermal layer is somewhat thicker in winter than in summer. This is especially true in the region between 8° N. and 12° N., where the summer isothermal layer almost reaches the surface and the winter isothermal layer is much thicker. The characteristic features of the latitude dependence of the isothermal layer in this area agree fairly well with Reid's density model (Reid, 1948a, b). Near the Equator the isothermal layer has a thickness of about 100 m or more where it tends to tilt northward, first gradually, then rather sharply, reaching the shallowest depth at about 10°–12° N. in the summer months and at about 8°–10° N. in the winter months. If we accept the generally recognized theory that the shallowest isothermal layer coincides with the northern boundary of the Equatorial Countercurrent, then the thermal boundary lies somewhat more to the north than the boundary of our wind structure and, hence, the boundary of our computed current system (fig. 189). The difference in the positions of the shallowest isothermal layer for winter and summer sections from the Japanese results probably indicates the seasonal shift of the Countercurrent system. Commencing at latitude 10°–12° N., the isothermal layer dips rather sharply to the north, which means a deeper layer in the North Equatorial system than in the Countercurrent system.

Sverdrup and others (1946, p. 708) also noted that the thickness of the isothermal layer in the North Pacific increases from east to west. Owing to the relatively small east-to-west coverage of the area under study, however, no longitudinal variation was detected in this area.

The thermocline layer, which was indicated by the large gradient in the temperature profile in figure 191 and by the crowding of isotherms in figure 192, lies in general between 75 m and 300 m, an average of about 200 m for the area as a whole. The general tendency of isotherms in this layer is to lie nearly parallel to the isotherms in the isothermal layer. However, the position of the shallowest thermocline layer apparently shifts to the south; it appears, at about 5°–8° N. in the Crossroads section and at about 6°–9° N. in the Japanese sections. These positions correspond fairly well with the northern boundary of the Countercurrent as established by dynamic computations. The hump-shaped isotherms which indicate a lower temperature at each relevant depth, in the northern boundary of the Countercurrent, probably

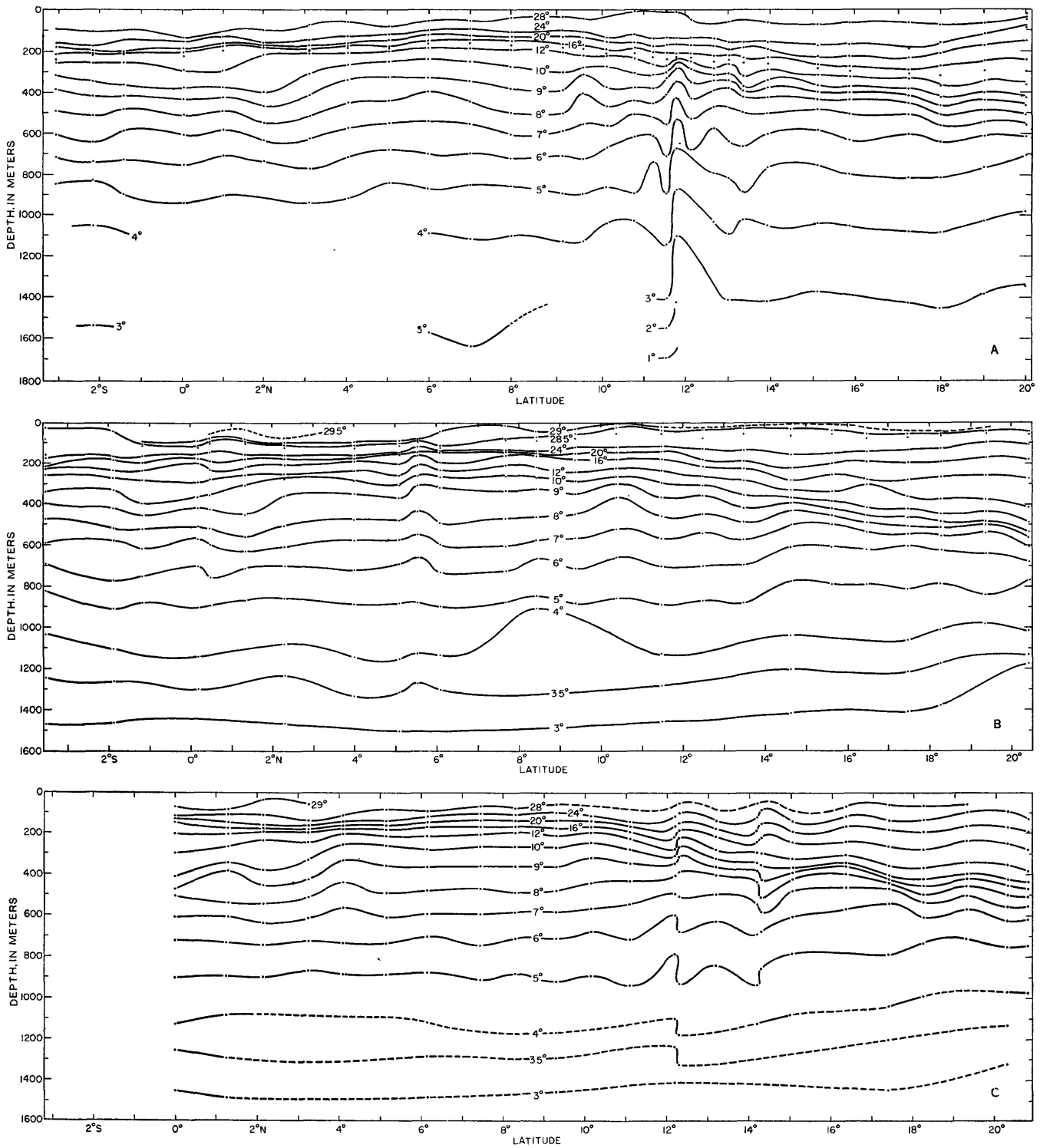

FIGURE 192.—Vertical distribution of temperature. *A*, From Crossroads data, March to August 1946. *B*, From Japanese data, 1933–41, summer season. *C*, From Japanese data, 1933–41, winter season.

suggest that the vertical motions which were treated by Defant (1936) and Yoshida and others (1953) are not limited to the upper mixed layer only but might penetrate quite deeply into the thermocline layer. This phenomenon of lowering temperature in the northern boundary of the Equatorial Countercurrent is a characteristic feature which we shall discuss further with the horizontal distributions of temperature.

Another noticeable feature deserves mention in discussion of the thermocline layer. In the Crossroads section (fig. 192*A*) a sharp dip appears in the isotherms of 12° C and 10° C near the Equator, thus causing the thermocline layer to be much thicker there. This feature was explained by Barnes and others (1948) as an intrusion of the South Pacific Water. A similar, yet less distinctive, feature also appears in the Japanese sections, but the positions of the dip and the isotherms in which the dip appears are somewhat different; this probably suggests that the intrusion of the South Pacific Water varies considerably in its extent and in its depth.

Descending from a depth of about 300 m, the vertical temperature gradient is generally so slight that the isotherms in the vertical sections become farther and farther apart. The characteristic features of isotherms in the two upper layers generally disappear at this layer. Some quite drastic changes of temperature in the neighboring stations are thought to be of a local nature and therefore of no general significance. The quite wavelike trend in the deeper isotherms can be largely attributed to the fact that below the thermocline the vertical temperature gradient is so slight that it is very difficult to be sure of the exact depth of a scaled value of temperature. Neglecting their wavelike variations, the isotherms of this layer are largely horizontal, which means that latitude does not play too strong a role in temperature distributions. A temperature of 3° C was observed in both the Crossroads and the Japanese investigations.

It may be of some interest to note that near the Equator the dips of isotherms appearing in the thermocline layer extend even to this depth. In the Crossroads section (fig. 192*A*), it is clearly seen that this dip appears distinctly at a depth as great as that of the 6° C isotherm (about 800 m) and in the Japanese sections as deep as the 7° C isotherm (about 700 m). Furthermore, the position of this dip shifts more and more to the north with increasing depth. This probably suggests that the component of the intrusive South Pacific Water becomes ever larger with increasing depth. As we shall see later, owing to the higher salinity of South Pacific Water, its density is naturally higher; therefore, it should underlie the North Pacific Water.

Three profiles of vertical salinity distribution from the Crossroads data and from the Japanese data along the same longitudes as for the temperature are shown as figure 193. In an attempt to explain the profound characteristic features in these figures, a brief mention of the salt concentration associated with the major water masses in this area is necessary. From a first glance at these three sections, it is immediately seen that the vertical salinity distribution is characterized by a pair of high-salinity tongues and a pair of low-salinity tongues, both coming from north and south. A detailed discussion of the properties of water masses could not be properly presented until the temperature-salinity (T–S) relationships are duly analyzed, but it should suffice to say here that the two tongues of high salinity and the two tongues of low salinity represent the saline Tropic Water and fresh Intermediate Water, respectively.

The Tropic Waters (Upper Water masses) acquire their characteristic properties at the air-sea boundary in the tropical area, where the evaporation is usually high and hence where salinity is high. Since Tropic Water is warm, its density is not great, and therefore only the warm and fresh Equatorial Water may overlie it. The depth of the salinity maximum, which roughly corresponds to the central axis of the two saline Tropic Waters, lies at a depth of about 150 m and is nearly horizontal. Comparing the northern and the southern tongues, the southern is the more saline. The maximum salinity reaches 35.60°/₀₀ to 35.80°/₀₀ in the southern tongue, while in the northern tongue it rarely exceeds 35.30°/₀₀. The vertical salinity gradient from the surface to salinity maximum is exceedingly high in some places; for instance, the Crossroads section (fig. 193*A*) shows that in the vicinity of the Equator salinity increases more than 1.4°/₀₀ at an interval of about 100 m (from 34.20°/₀₀ at about 50 m to more than 35.60°/₀₀ at about 150 m), which is a very large gradient of salinity in the open ocean.

In contrast to the characteristic properties of the Tropic Waters, the Intermediate Waters are characterized by their low temperature and low salinity. These properties were acquired at their sources (North and South Subpolar areas) where the air temperature is low, precipitation high, and the salinity therefore low. In spite of their low salinities, their densities are high because of their low temperatures. Naturally they underlie the Tropic Waters and occupy the intermediate depth, whence their name. The depth of the central axis of minimum salinity varies greatly with latitude. As we have previously noted, the southern tongue is the deeper. Near the Equator, the salinity minimum may appear as deep as 800 to 1000 m, and the value of salinity is almost uniformly close to 34.50°/₀₀. The inclination with latitude of the central axis of the

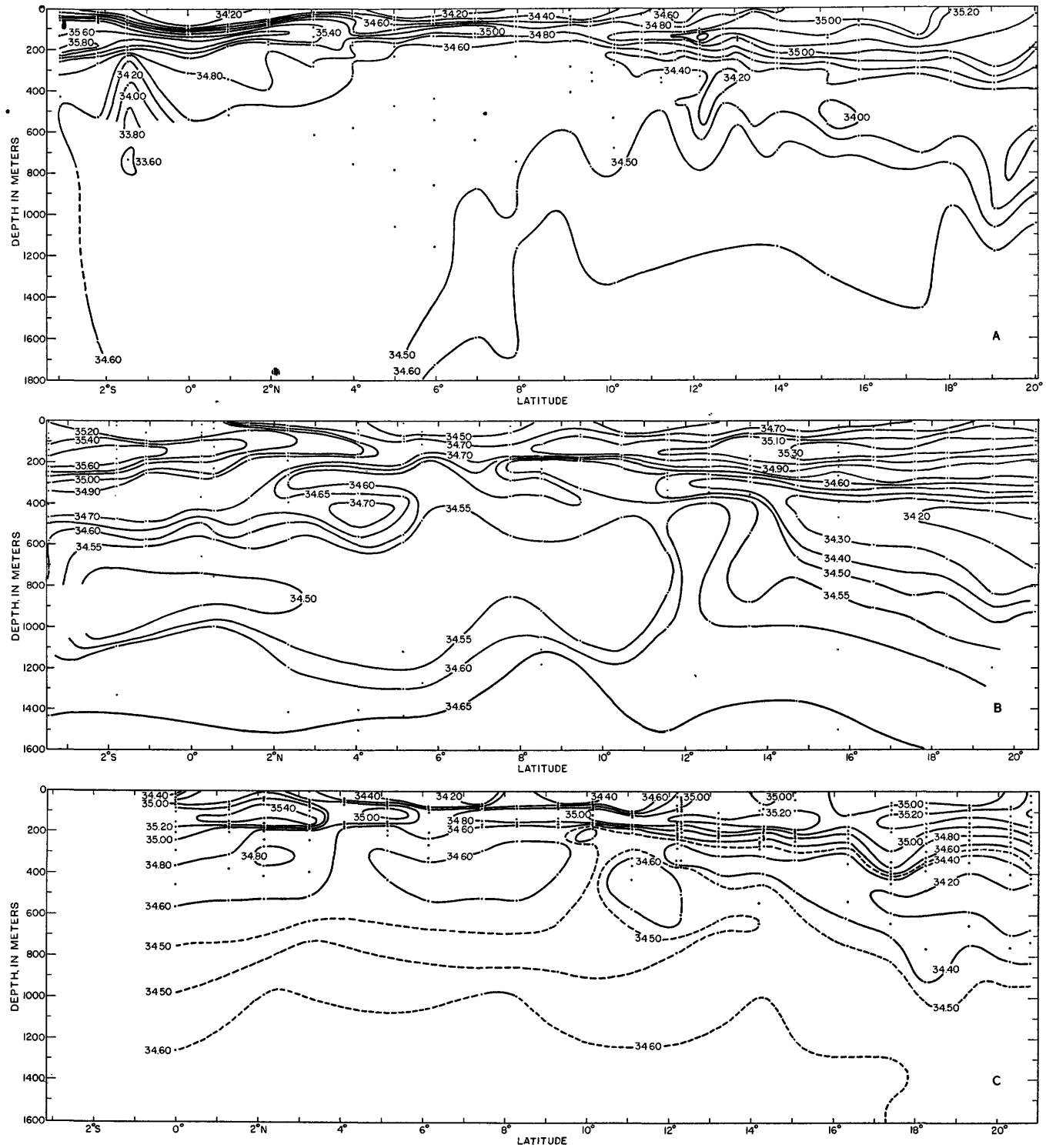

FIGURE 193.—Vertical distribution of salinity. *A*, From Crossroads data, March to August 1946. *B*, From Japanese data, 1933–41, summer season. *C*, From Japanese data, 1933–41, winter season.

315915—55——4

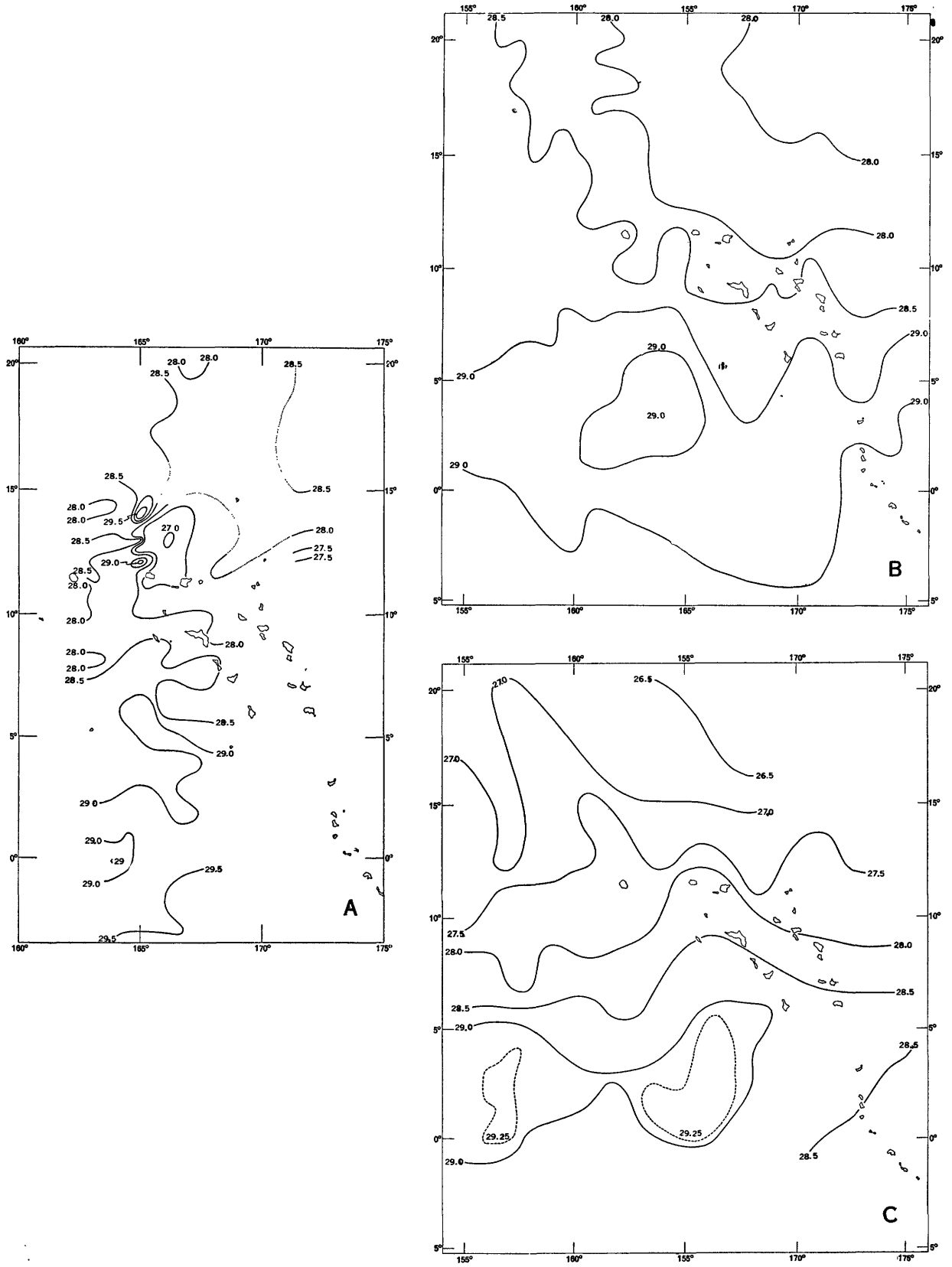

FIGURE 194.—Horizontal distribution of temperature at surface. *A*, From Crossroads data, March to August 1946. *B*, From Japanese data, 1933–41, summer season. *C*, From Japanese data, 1933–41, winter season.

Southern Intermediate Water is slight yet perceptible. On the contrary, the inclination of the central axis of the Northern Intermediate Water is tremendous, lying at a depth as great as 500 to 600 m at 20° N. and rising almost linearly to a depth of 150 to 200 m at 8°–10° N. This inclination of axis probably suggests the ascending of the North Intermediate Water with decreasing latitude because of the fact that the density in this water mass decreases owing to the "warming-up" of the water mass through mixing with the surrounding water masses on its long journey. The associated salinity of this water mass is also somewhat increased from 34.00‰–34.20‰ at 20° N. to 34.50‰ at 8°–10° N.

The region at about 6°–10° N. roughly corresponds to the eddy area which we mentioned in the discussion of water circulation, acting as a "baffle" or a "transitional" zone between the northern and southern tongues. No appreciable salinity maxima and minima appear there. Consequently the salinity gradient is relatively weak.

HORIZONTAL DISTRIBUTION

AT THE SURFACE

The horizontal distribution of the surface reversing-thermometer temperatures from the Crossroads data and the Japanese data are shown as figure 194. It is to be noted that at the sea surface as well as in the upper mixed layer, water temperature is primarily affected by such ever-varying local boundary conditions as heating, cooling, evaporation, and local wind. The characteristic property of the surface-temperature distribution is not so clear as that in deeper layers where water temperature is essentially associated with water-mass properties and water circulations. However, some noticeable features which can be derived from these figures and need to be briefly mentioned are:

1. In general, the surface temperature in this area decreases slowly with increasing latitude, though the horizontal gradient is very slight.

2. Intensive upwelling associated with Equatorial divergence is thought to occur at and near the Equator; thus the surface temperature there should be somewhat lowered. This feature is clearly seen in the two figures (fig. 194*A*, *B*) for the summer months. In the winter season, from the Japanese results, this feature is not evident.

3. A tongue of cool water, roughly corresponding to the cool-water tongue from the northeast mentioned by Robinson (1954) appears in all three figures in somewhat different latitudes. In an attempt to explain the origin of the cool-water tongue from the northeast, Robinson suggested it might be associated with the ascending motion in the northern boundary of the Countercurrent. The temporal and spatial variations of its position might be due to the change of such external boundary conditions as winds.

The characteristic features of surface-salinity distribution as shown in figure 195 are much more distinctive than those of surface temperature. Bands of low salinity appear generally in the same area of large eddies. Their respective positions are at about 4°–6° N. from the Crossroads data (fig. 195*A*) and at about 6°–8° N. from the Japanese data (fig. 195*B*, *C*). From both sides, waters of higher salinity push toward this band of low salinity. The larger gradient on the southern side probably suggests that the strongest invasion comes from the southwest sector—from the Southern Hemisphere.

AT THE 100-METER LEVEL

The horizontal distributions of temperature and salinity at the 100 m level are shown as figures 196 and 197, respectively. The temperature distributions at this level differ fundamentally from those at the surface. Whereas at the surface there exists no close connection between the distributions of these two properties, an obvious resemblance now appears at this level. Comparing figures 196 and 197, it is easily seen that in the area of large eddies distinctive bands of low temperature and salinity occupy nearly the same area. Recalling the fact that the density of sea water is, in general, a mirror image of the water temperature, then the band of "dynamic low" (the high density) in the geostrophic flow may be simply a reflection of the band of low temperature. To determine the reality of the horizontal large eddies in this region, more direct measurements of the current are needed.

AT THE 250- AND 300-METER LEVELS

For the representation of the intermediate level, different depths were used. This is due to the fact that in the processed data of the Crossroads and the Japanese results, values of temperature, salinity, and pertinent factors were scaled at these different "standard depths." To avoid the tedious and time-consuming work of reprocessing, it is found necessary to use different depths. However, this representation has no appreciable effect on our conclusions since the major features of temperature and salinity distributions at these depths are essentially the same.

With the exception of a few minor changes, the characteristic features of the distribution of temperature (fig. 198) and salinity (fig. 199) at these depths remain practically unchanged from those at the 100 m level. A noticeable feature is that the band of low temperature is enlarged at this level in comparison to the 100 m level. This agrees with our earlier statement that the size of the large eddies increases with increasing depth.

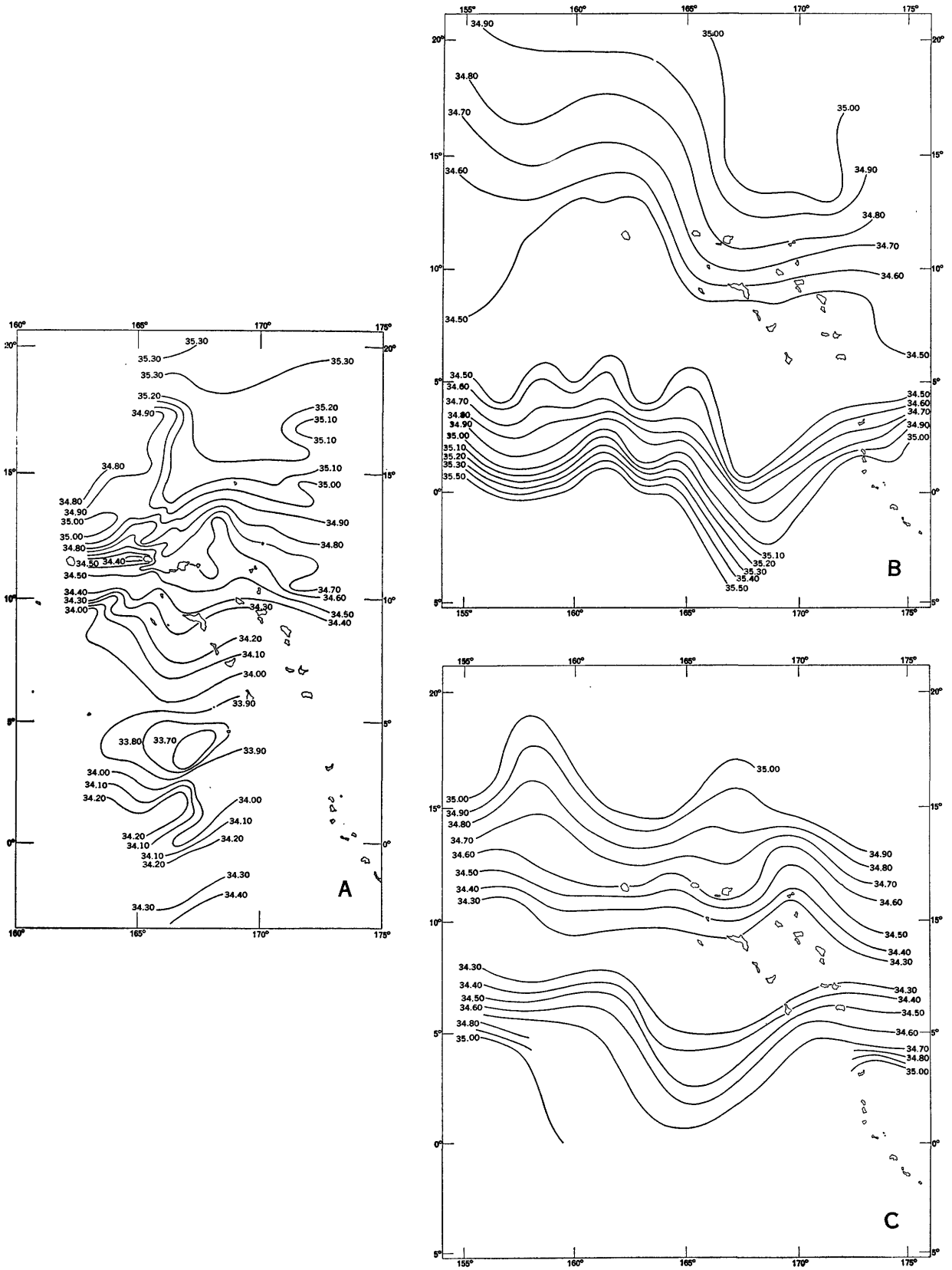

FIGURE 195.—Horizontal distribution of salinity at surface. *A*, From Crossroads data, March to August 1946. *B*, From Japanese data, 1933–41, summer season. *C*, From Japanese data, 1933–41, winter season.

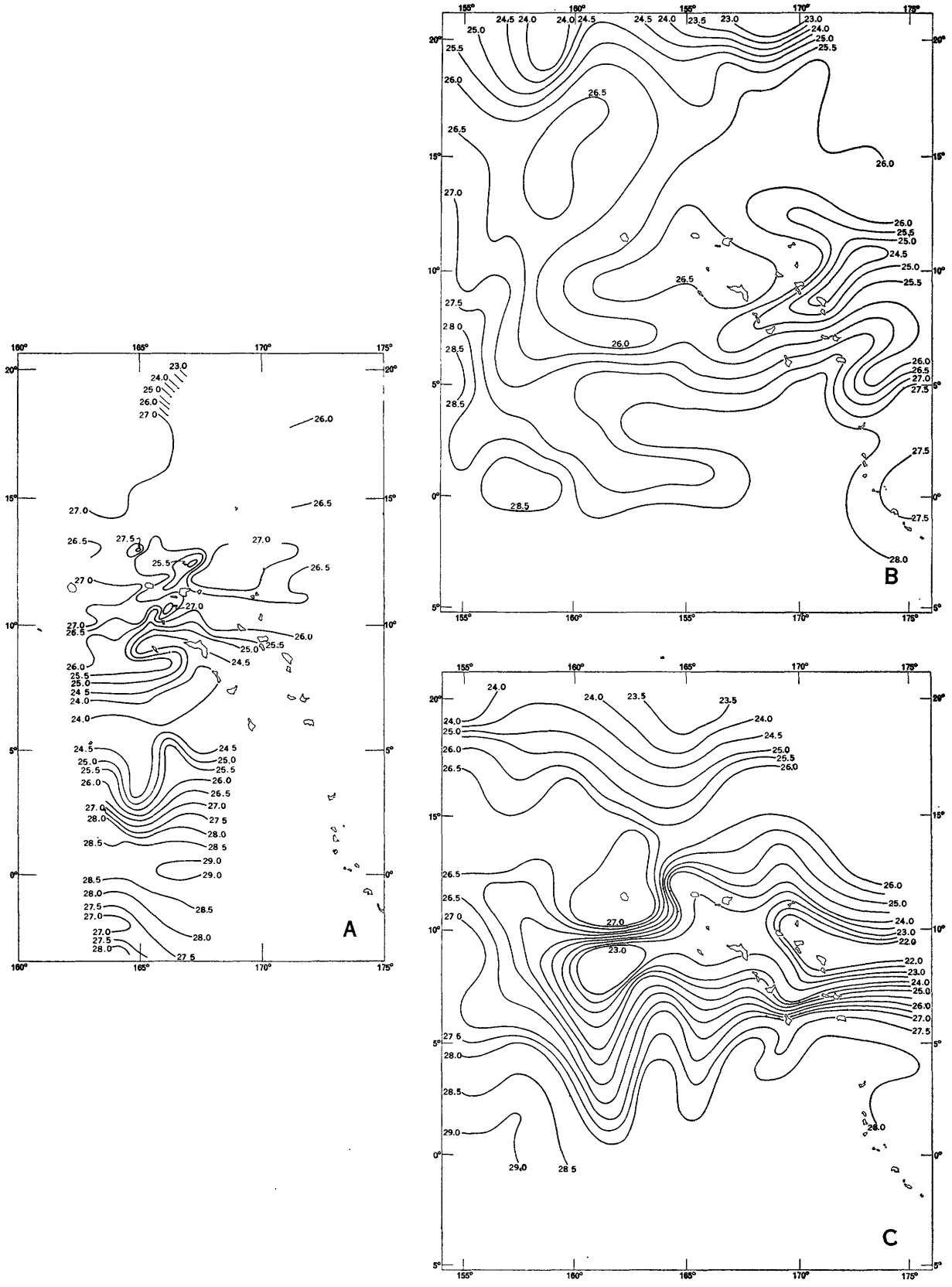

FIGURE 196.—Horizontal distribution of temperature at 100 meters. *A*, From Crossroads data, March to August 1946. *B*, From Japanese data, 1933–41, summer season. *C*, From Japanese data, 1933–41, winter season.

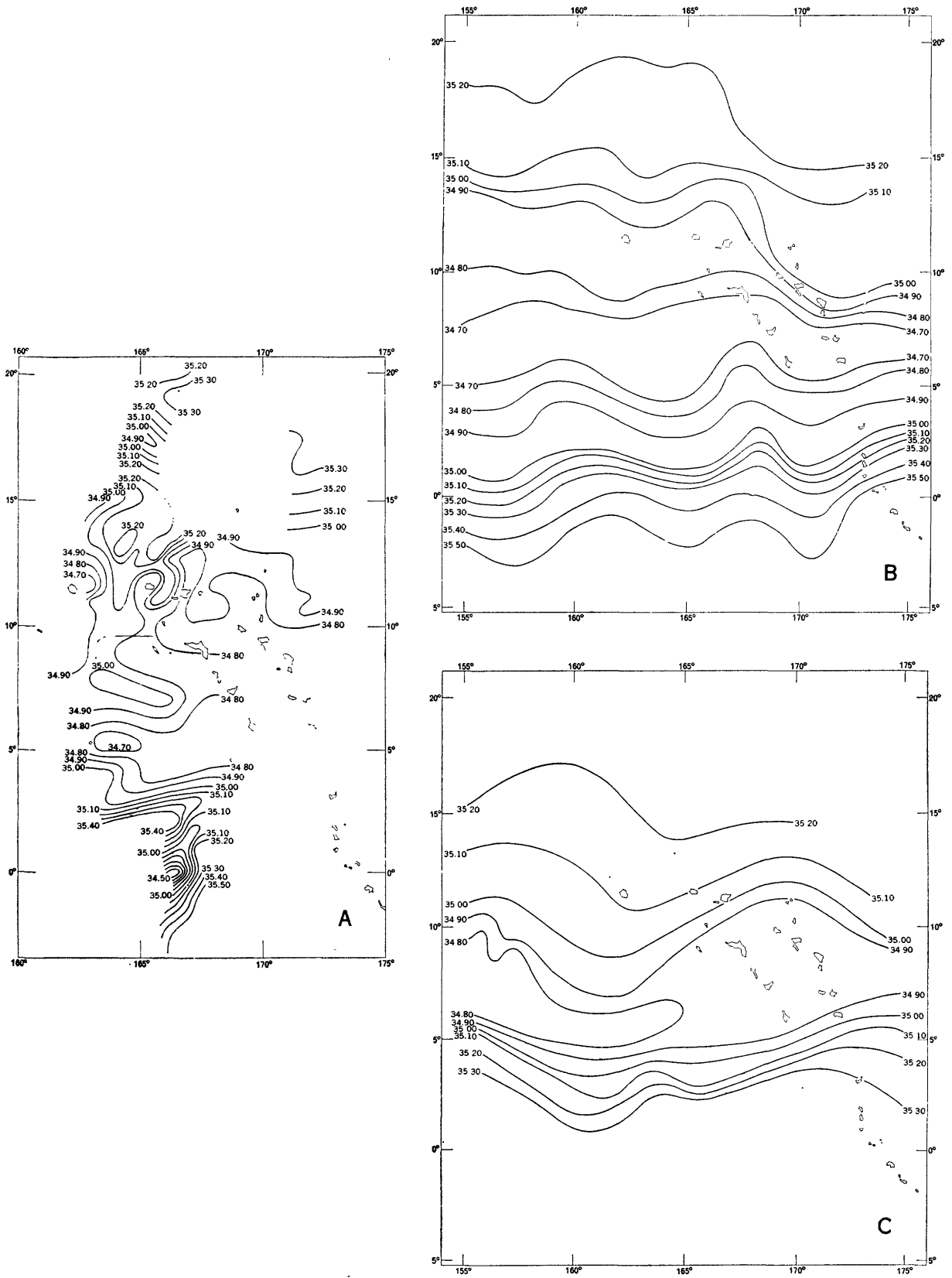

FIGURE 197.—Horizontal distribution of salinity at 100 meters. *A*, From Crossroads data, March to August 1946. *B*, From Japanese data, 1933–41, summer season. *C*, From Japanese data, 1933–41, winter season.

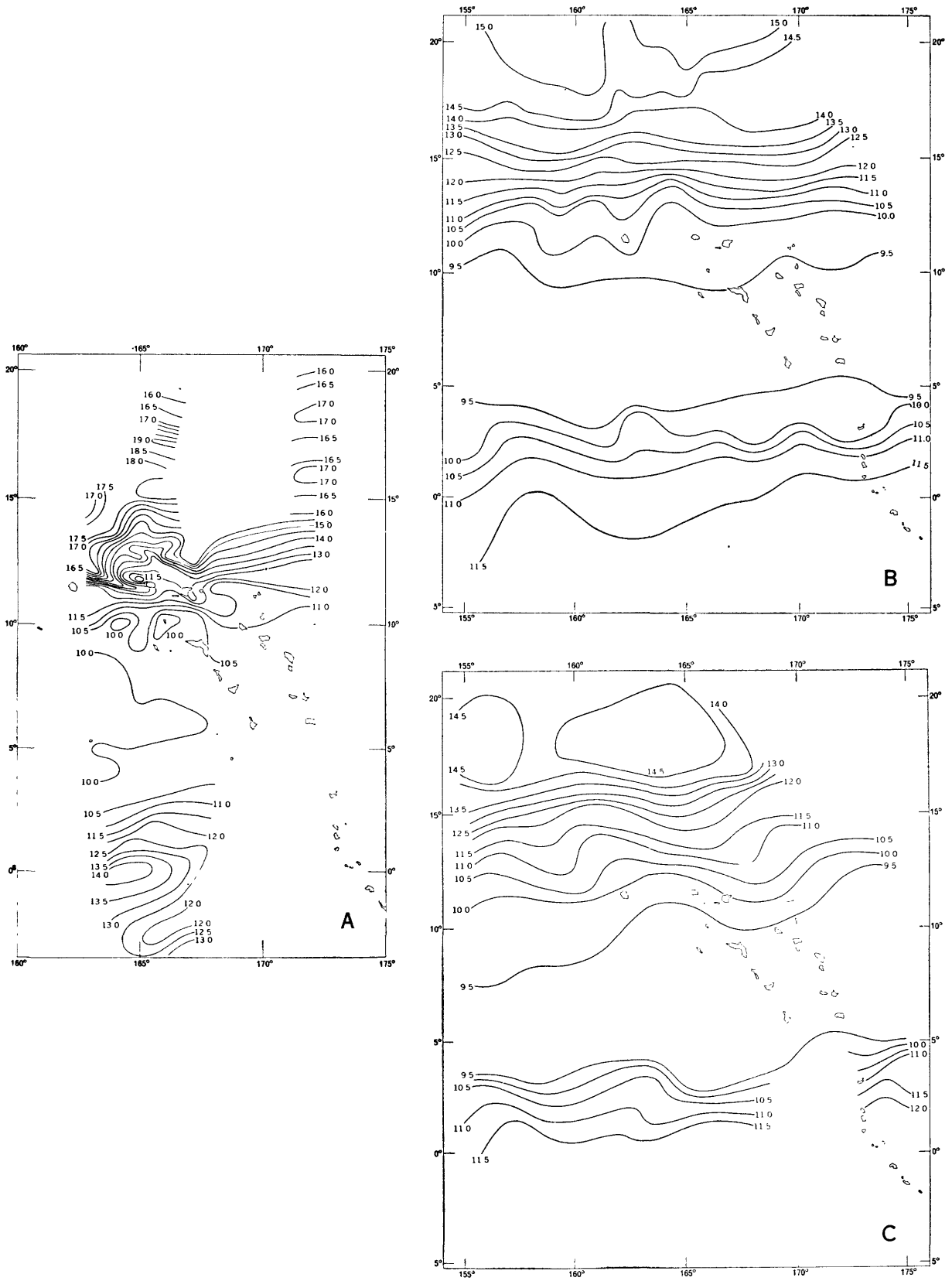

FIGURE 198.—Horizontal distribution of temperature. *A*, At 250 meters, from Crossroads data, March to August 1946. *B*, At 300 meters, from Japanese data, 1933–41, summer season. *C*, At 300 meters, from Japanese data, 1933–41, winter season.

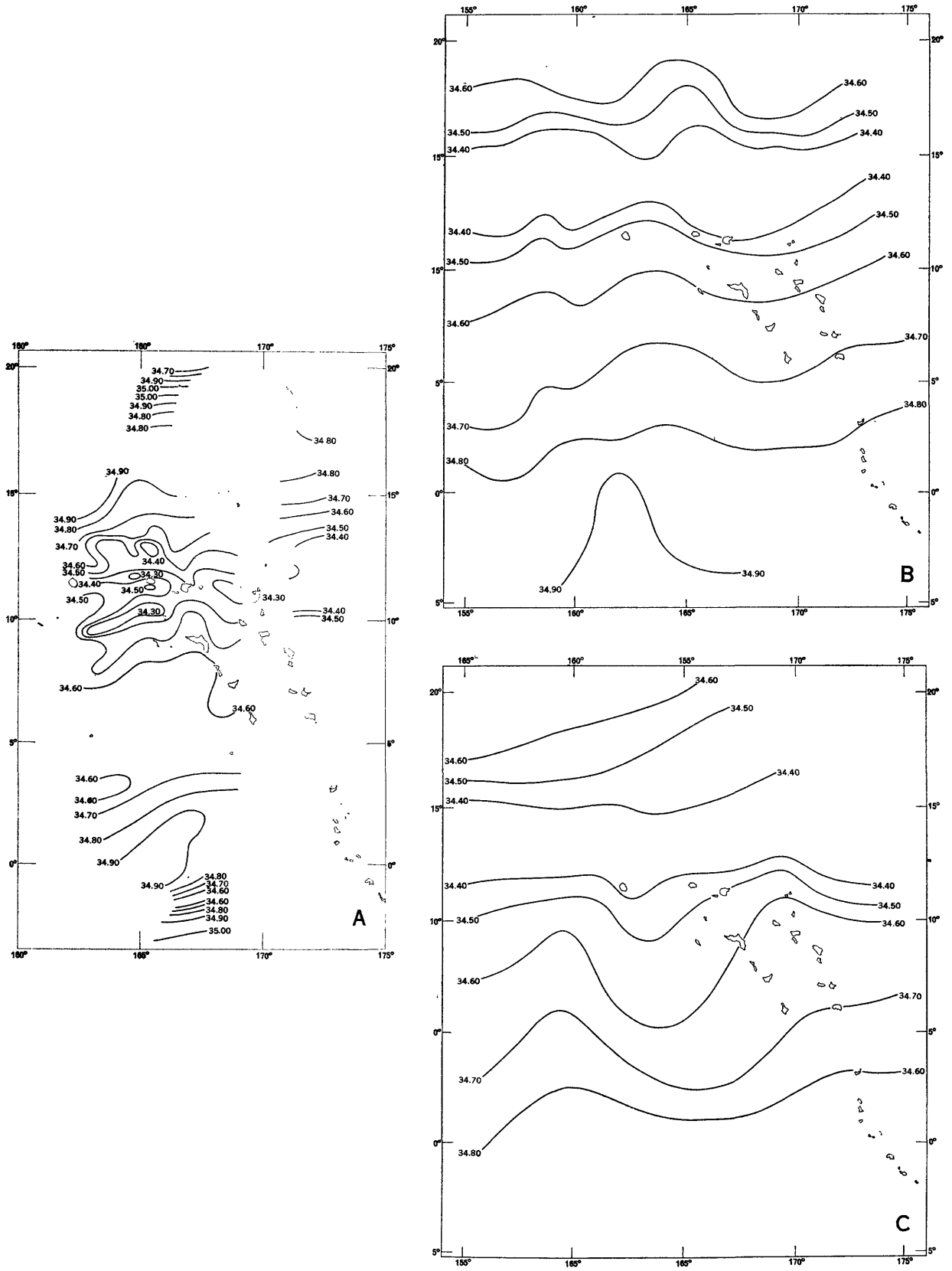

FIGURE 199.—Horizontal distribution of salinity. *A*, At 250 meters, from Crossroads data, March to August 1946. *B*, At 300 meters, from Japanese data, 1933–41, summer season. *C*, At 300 meters, from Japanese data, 1933–41, winter season.

In the distribution of salinity it is noticeable from both the Crossroads and the Japanese data that the band of low salinity which appears at about 6°–8° N. at 100 m, now shifts to the north of 10° N. at this lower level. Recalling our previous statement as to the inclination of the axis of salinity minimum (of Intermediate Water), the shift is easily understood. From figure 193*B* we can immediately see that at the 250 m–300 m level, the area at about 10°–14° N. is right at the axis of the salinity minimum, whereas the area south of it is above and the area north of it is below the salinity minimum at this depth.

AT THE 500-METER LEVEL

Two features characterize the horizontal distribution of temperature at the 500 m level (fig. 200): (1) the band of low temperature at the area of the large eddies is still somewhat recognizable, but very faint, and (2) the axis of lowest temperature at this level moves northward to about 13° N., from the Crossroads data, and to about 15° N., from the Japanese data.

The main feature of the distribution of salinity at this level (fig. 201) is that the center of low salinity moves farther northward. The northern region, which was an area of high salinity in the upper levels, now becomes the center of low salinity.

These features in the distribution of both temperature and salinity can be similarly attributed to the fact that the axis of the Intermediate Water is inclined. It is clearly seen from figure 193*A* that as depth increases the area of southern latitudes is already out of the center of the Intermediate Water, only the northern area being within its central axis.

CONCLUDING REMARKS

Concluding the discussion of the spatial (vertical as well as horizontal) distributions of temperature and salinity of the Marshall Islands area, it is noted that

1. With the exception of the surface temperature, the most outstanding feature of the distribution of temperature and salinity for the upper 250 m–300 m layer is the appearance of a band of low temperature and low salinity in the area at about 5°–10° N., or approximately the area of the large eddies.

2. The primary causes of this outstanding feature are thought to be

a. High precipitation.

b. Absence of saline Tropical Water tongue from both north and south.

c. Ascending of the North Intermediate Water mass with decreasing latitude, thus enabling the cool and fresh water associated with this water mass to come up to a level which in all other areas is occupied by warm and saline (northern and southern) Tropical Water masses.

d. Upwelling associated with mean current (Defant, 1936; Yoshida and others, 1953).

e. Upwelling associated with cyclonic eddies (Uda, 1940; 1949; 1952).

It is reasonable to assume that both types of upwelling originate at some intermediate depth, thus bringing cool and fresh water into the upper levels. The pushing and ascending of both the northern and southern Intermediate Water masses may further strengthen this upwelling.

SEASONAL VARIATIONS

A detailed discussion of seasonal variations of temperature and salinity from month to month is not possible in this study. For several months no observational data were available from either the Crossroads or the Japanese data, and in some other months the number of data available was so small that their statistical value is questionable. Therefore the phrase, "seasonal variation," which we adopted here according to usage, in actuality only means the difference of average temperature or salinity between the summer months (April to September) and the winter months (October to March). All values of temperature and salinity within 2° of latitude interval were averaged together for each season. No account is taken for the longitudinal difference. For the sake of brevity, the area with an average value of temperature or salinity in the summer season larger than that in the winter season is named the "positive area"; the area where the average value of temperature or salinity is smaller in summer than in winter is termed the "negative area."

Figures 202 and 203 present the major features in seasonal variations of temperature and salinity in the upper 100 m level. Since the seasonal variation of both quantities below the 100 m level is rather confusing, no definite features can be traced; therefore, we shall not mention them here. In an attempt to interpret the profound characteristic features in figures 202 and 203, the following suggestions are proposed:

The striking parallelism of both temperature and salinity variations for the upper 50 m level and the remarkable difference between the 100 m curve and other curves for both temperature and salinity strongly indicate the influence of a discontinuity surface—that is, the thermocline or the interface of the upper mixed layer and the underlying layer, exerted on the vertical distribution of temperature and salinity above and below this surface. Our previous statements as to depths of this discontinuous surface—that it varies with latitude considerably and that it averages about 75 m for the whole area considered—are further con-

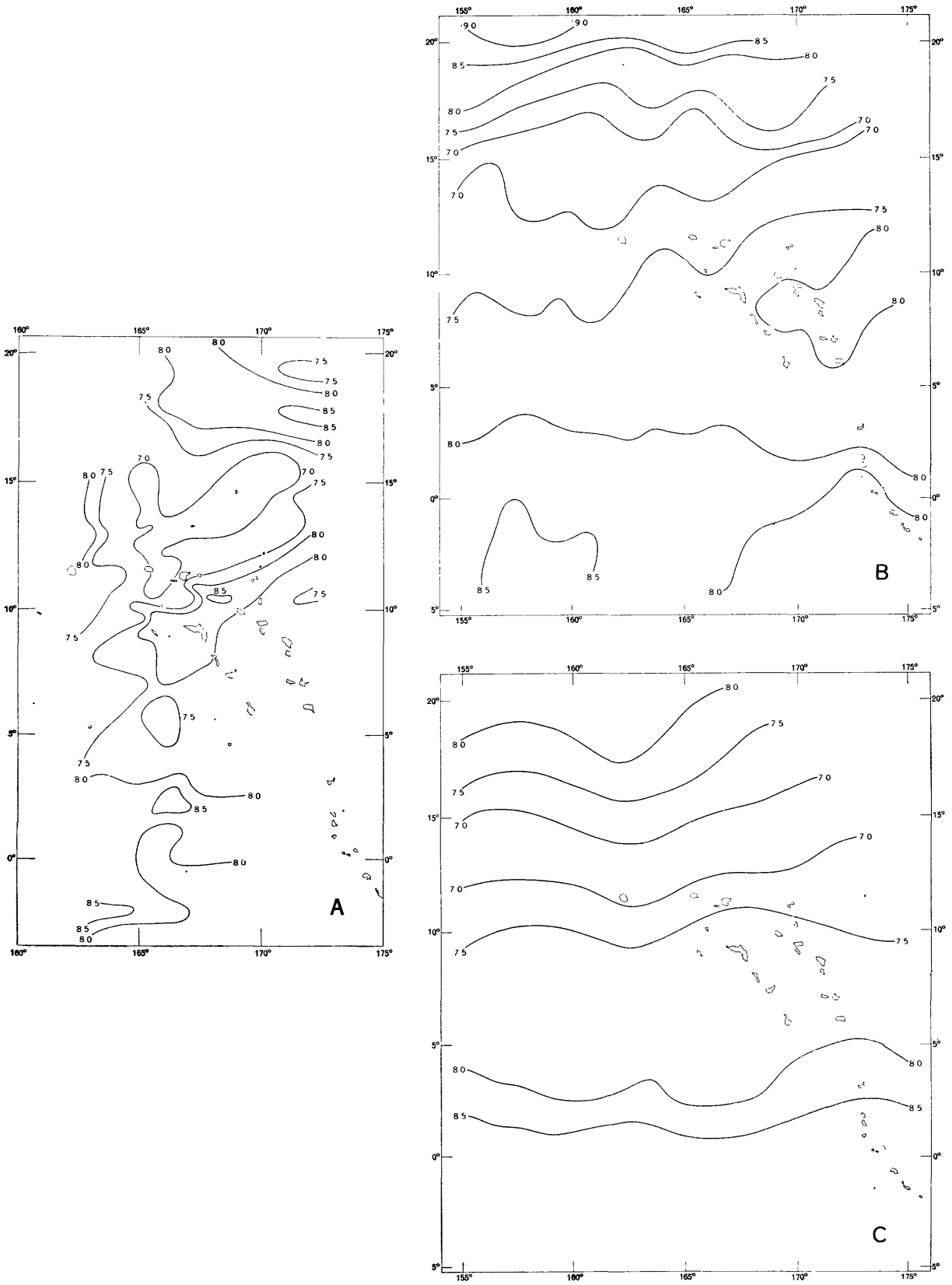

FIGURE 200.—Horizontal distribution of temperature at 500 meters. *A*, From Crossroads data, March to August 1946. *B*, From Japanese data, 1933–41, summer season. *C*, From Japanese data, 1933–41, winter season.

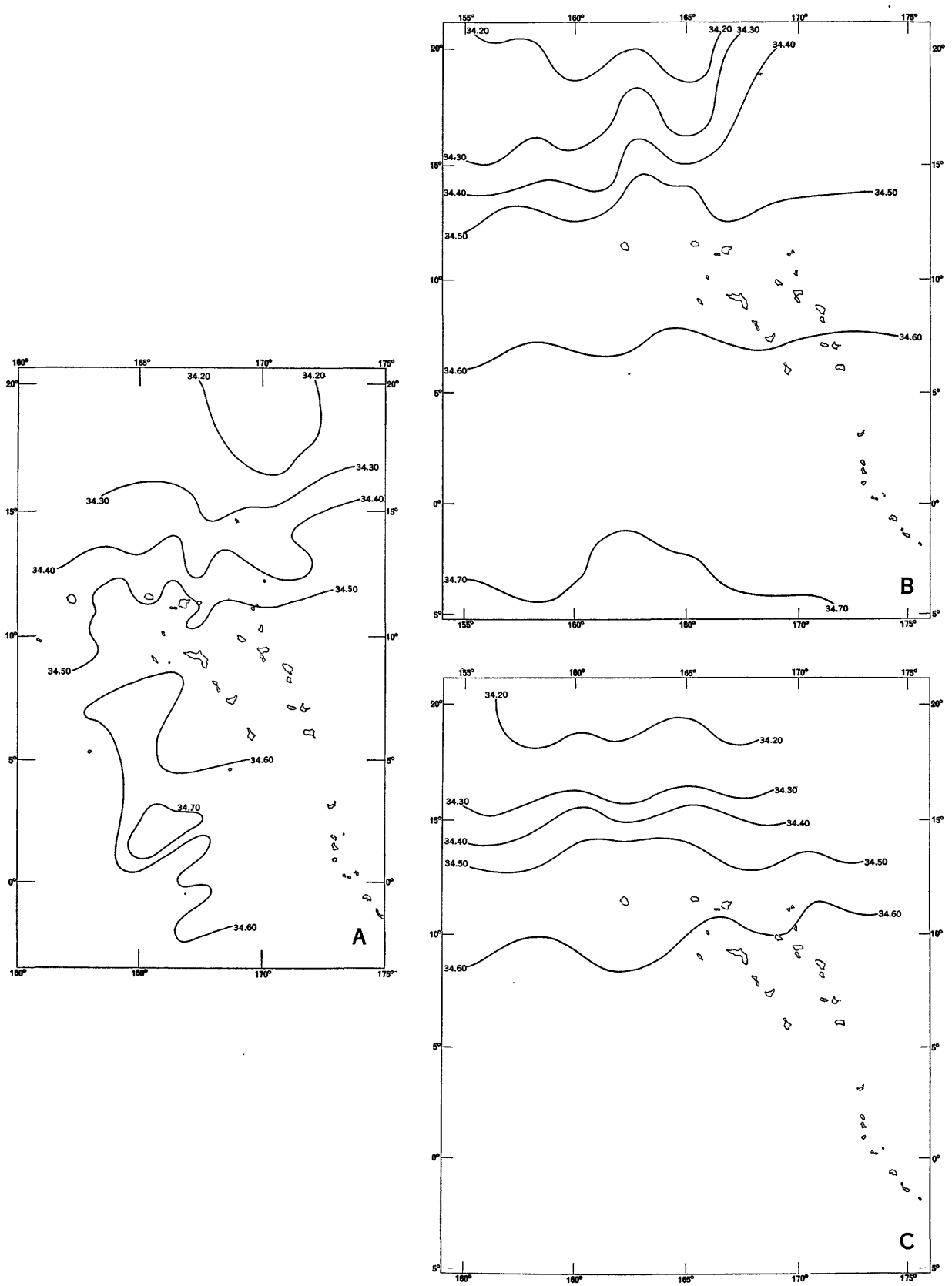

FIGURE 201.—Horizontal distribution of salinity at 500 meters. *A*, From Crossroads data, March to August 1946. *B*, From Japanese data, 1933–41, summer season. *C*, From Japanese data, 1933–41, winter season.

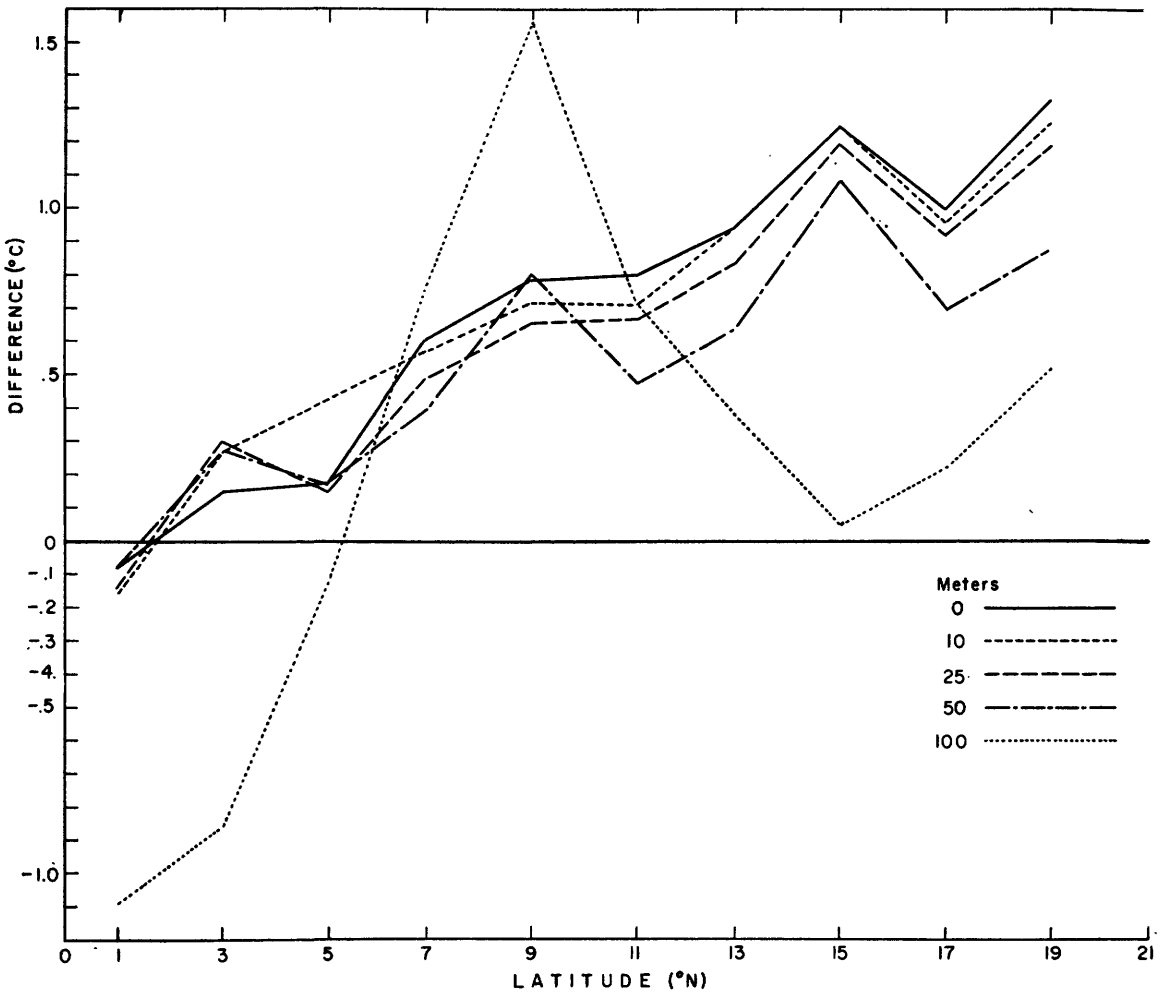

FIGURE 202.—Seasonal variation of temperature in the upper mixed layer, from Japanese data, 1933–41.

firmed by the trend of the curves in these two figures.

The approximately linear increase of temperature in the upper mixed layer with increasing latitude probably reflects the latitudinal dependence of seasonal variations in radiation.

The salinity positive area—that is, the area where summer salinity is higher than winter salinity—at about 7°–14° N. in figure 203 cannot possibly be due to the seasonal variation of evaporation because, in general, the evaporation at the sea surface is higher in winter than in summer. A rough calculation of seasonal variation of evaporation at these latitudes shows that the evaporation in winter is about twice as high as that in summer. It should, however, be noted that the absolute values of evaporation at these latitudes are comparatively low even in the winter season (Jacobs, 1951). This suggests that a negative area—that is, an area where summer salinity is lower than winter salinity—instead of a positive area should appear there if evaporation is an important factor. A possible seasonal shift of the position of the Countercurrent system may likewise have an unfavorable effect. As we have shown in the previous sections, the northern boundary of the Equatorial Countercurrent is an area of fresh water; a shift to the north of that fresh water in the summer would also reduce the summer salinity. Thus a negative area would appear in the seasonal variation of salinity.

It is thought that the appearance of a salinity negative area (at about 1°–7° N.) and a salinity positive area (at about 7°–14° N.) side by side in figure 203 might be associated with the seasonal variation of the vertical motion and especially the upwelling. It seems reasonable from Robinson's work (1954) that both upwelling in the northern boundary and descending motion in the southern boundary of Equatorial Countercurrent are more intense in winter than in summer. Uda (1940, 1949, 1952) in his study of cold water in the Japan Sea also pointed out that the type of upwelling associated with cyclonic eddies is also stronger in winter when the stability of sea water is slight. As we previously men-

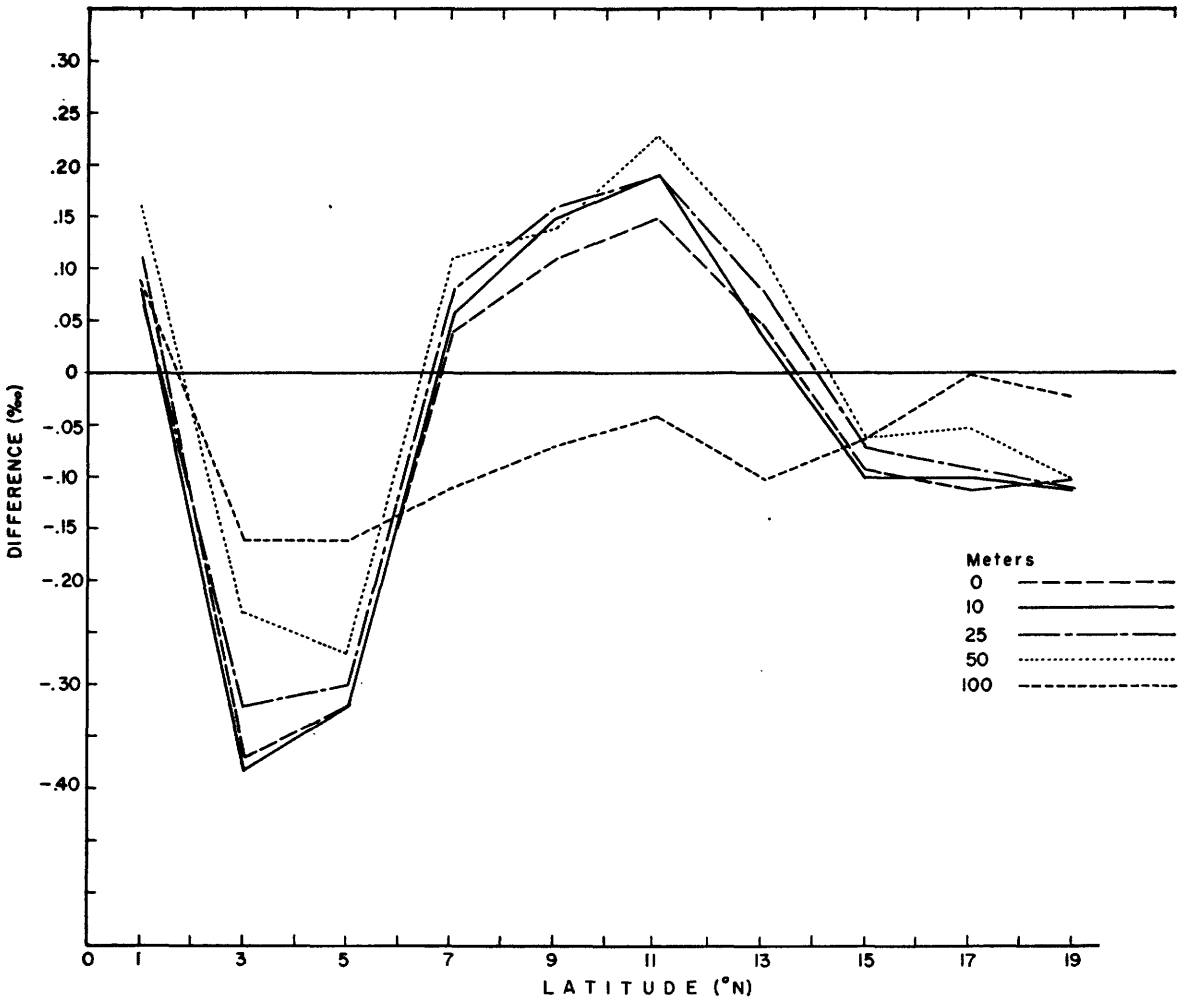

FIGURE 203.—Seasonal variation of salinity in the upper mixed layer, from Japanese data, 1933–41.

tioned, both types of upwelling were thought to originate at an intermediate depth where both temperature and salinity are low. The stronger upwelling of both types in winter means that more cool and fresh water is brought up to the topmost layer in that season, thus reducing the winter salinity and causing a positive area in the northern boundary of the Countercurrent. The intense descending motion in the southern boundary of the Countercurrent in a winter has a reverse effect generally and therefore may cause a negative area in the lower latitude.

It is thought that the cooling and warming effects which are exerted on the seasonal variation of temperature in the topmost layer by respective upwelling and descending motion is largely covered or masked by the seasonal variation of radiation.

DISTRIBUTION OF DENSITY

In discussing the distribution of density, only the Crossroads data are available, because the values of σ_t have not been included in the computations from the Japanese data. Consequently the prepared figures of density distributions are not detailed enough to be discussed at length.

The distribution of density of sea water, customarily represented by values of σ_t, is solely determined by the distribution of temperature and salinity, which have been discussed in the previous sections. This section, therefore, is intended only to draw attention to the general features of the density distributions in this area.

In dealing with the distribution of density, it should be of particular interest to keep the interrelationship between mass and current in mind. It is expected that the general rule for mass-current relationship can be satisfied as far as our computed current system is concerned. Although, especially at the levels near the surface, the actual current may differ somewhat from such geostrophic flow, knowledge of vertical distribution of density is still essential to the discussion of the currents. In this connection it may be desirable that the vertical profile of density from our data (fig. 204) be compared with Reid's density model (Reid, 1948b).

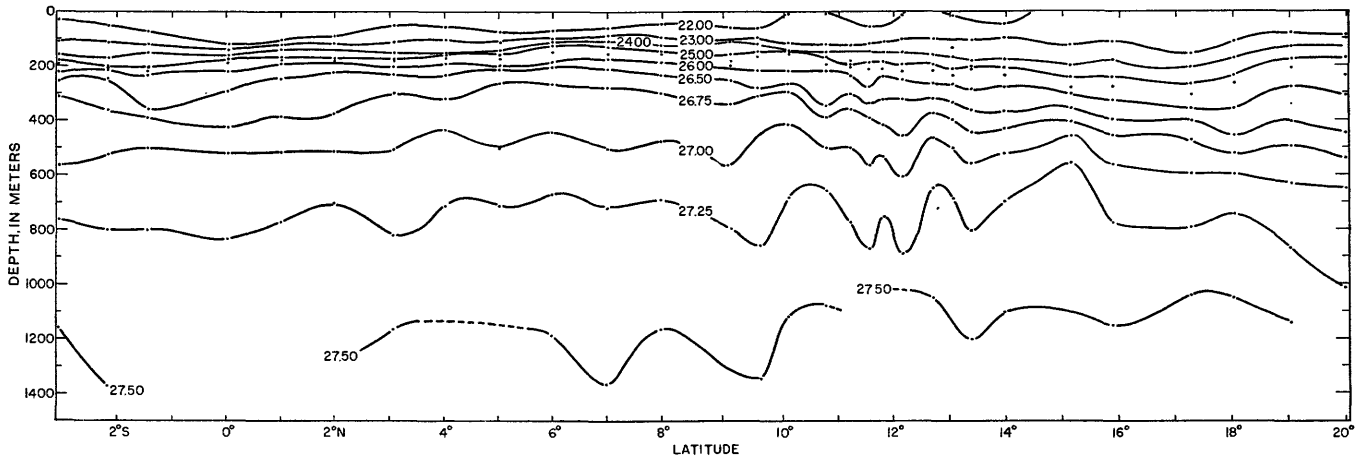

FIGURE 204.—Vertical distribution of density (σ_t values), from Crossroads data, March to August 1946. In order to avoid overcrowding of contours in the shallower layers unequal contour intervals have been used in this figure.

Only a rough comparison with Reid's model indicates a somewhat essential difference from the Carnegie data. It is interesting to note that the vertical profile at 5° N. from our data is similar to that of the Carnegie at 10°–12° N., corresponding to the southward shift of the wind characteristics.

As was mentioned before, it is seen that isopycnic lines largely follow isotherms in the relevant section. A detailed discussion of the depth of thermocline was given in the section on temperature distribution and is not entered into in this section.

AT THE SURFACE

[fig. 205*A*]

The most prominent feature of the density distribution at the surface is the appearance of an area of low density at about 5° N. This feature seems to be inconsistent with the general rule for mass-current relationship. According to the general rule an area of high density instead of low should appear in this area of the northern boundary of the Countercurrent. (See p. 647.) However, beneath the surface in this area, water of the highest density exists, as will be mentioned later. This is in good accordance with the Carnegie data. Actually, however, in the surface layers the relationship between current and density is different from that inferred from the rule for geostrophic flow.

Comparing figure 205*A* with the chart of the horizontal distribution of salinity at the surface (fig. 195*A*) it is interesting to note that the agreement between distribution of salinity and that of density at the above area is remarkably good. This appears to suggest that the salinity distribution is the dominating factor in the distribution of the density at the very surface, mainly owing to the uniform horizontal distribution of the temperature in this area. This tendency is especially outstanding in the southern part of the area where the horizontal temperature gradient at the surface is almost negligible.

The density of water increases northward from the center of low density and the shape of isopycnic lines closely resembles that of isohalines. At about 14° N., northeast of Bikini Atoll, the density reaches its highest value, the natural consequence of the low temperature and high salinity there.

AT THE 100-METER LEVEL

[fig. 205*B*]

The horizontal distribution of density at the 100 m level is essentially changed from that at the very surface. This can be understood by the fact that the thickness of the surface isothermal layer is generally less than 100 m, as was mentioned in the previous section.

The area between 4° and 7° N. which corresponds to a region of low density at the surface is an area of high density at the 100 m level. This feature is similar to that indicated in the Carnegie data (Sverdrup and Fleming, 1944). The distribution of the major wind system in this area is south of the average location for the whole Equatorial Pacific. It may be of particular interest to pay attention to these features of density distribution in connection with those of wind distribution. An area of low density appears to be found in the area between 10° and 12° N., with local high density at about 13° N.

The agreement of the reverse relationship between the distribution of density and that of temperature is extraordinary. Areas of low density coincide with those of high temperature, while regions of high density are almost identical with those of low temperature. The predominant influence of temperature on the distribution of density is principally due to the high gradient of temperature at this level, which in most

cases lies within the thermocline layer. (See fig. 192*A*.) With the exception of the southernmost area, where an area of low density is located and directed in exactly the same fashion as that of the low salinity, the effect of salinity distribution on that of density is almost negligible. In this southernmost area, temperature gradient is not so large as in the northern parts.

AT THE 250-METER LEVEL

[fig. 205*C*]

An extensive area of high density, which follows exactly the area of low temperature between 2° and 7° N., constitutes the main feature of the distribution of density at this level. This feature appears to be ascribed to the Intermediate Water which extends above this level in this region and also to be related to the enlarged regions covered by horizontal eddies.

Density decreases rather rapidly northward from this high-density area. The lowest density is found at about 16° to 17° N. The density distribution in the southernmost part is unfortunately obscure because of the lack of salinity data.

AT THE 500-METER LEVEL

[fig. 205*D*]

At this level the distribution of density in the southern area (below 10° N.) is remarkably uniform; from 2° S. to 12° N., σ_t values at most stations lie in the neighborhood of 27.0. Commencing at 12° N., where the local high density is found, density decreases with increasing latitude. This may be essentially due to the regular northward decrease of salinity while the temperature distribution remains quite uniform (7.5° C) at this level in this area. The appreciable decrease of salinity in the northern area may be ascribed to the Intermediate Water, the core of which exists at this level in this area.

TEMPERATURE-SALINITY (*T–S*) RELATIONSHIP

GENERAL RELATIONSHIP

In previous sections we discussed the distributions of temperature and salinity separately, partly in connection with character of currents. The discussion in the present section is intended to make the interpretation of those distributions more clearly understood by use of the temperature-salinity (*T–S*) relationships, which may characterize water masses.

Observed temperature and salinity data are combined into groups for every 2° of latitude (in the area between 17° and 20° N., from the Crossroads data, the values over 4° of latitude have been grouped together because of scarcity of observations in those areas). T–S diagrams have been prepared respectively for each group from the Crossroads data and the Japanese data. In the diagrams, the mean curves of Western South Pacific Water (WSP), Equatorial Pacific Water (EP), and Western North Pacific Water (WNP) are reproduced as the reference curves after Sverdrup and others (1946, figs. 195, 196, and 199).

Three very distinct types of curves can be readily recognized from these groups of *T–S* diagrams. This situation is common to both the Crossroads and the Japanese data. Accordingly the area under study is divided into three regions for convenience of discussion.

Since the *T–S* relationship in the upper mixed layer is not considered conservative, discussion of it above 100 m is excluded here. Below about the 150–200 m level, generally well-defined water masses are present in all latitudes concerned, although the depth of the core of each water mass varies with latitude. It is noted that a transitional layer—corresponding approximately to the thermocline layer—appears between the surface-water mass and well-defined water masses below 200 m. A layer of salinity maximum, caused by the subsurface waters from tropical convergences, is present within the thermocline layer, and is shallowest at 8°–10° N., where the thermocline layer is also found to be the shallowest. It can be said that Western North Pacific Water covers almost all levels in the northern region, Equatorial Pacific Water covers almost all levels in the southern region, and in the central region stratification of these two waters is found.

As will be mentioned later, it appears that an Intermediate Water of northern origin is present at 300–500 m levels in the northern and central regions, with another Intermediate Water of southern origin at the 800 m level mostly in the southern and central regions. Thus, in the central region two maxima and minima of salinity are found, while in the northern and southern regions only one maximum and one minimum are seen.

Hence, the division of the area into these three regions may provide adequate information on the characteristics of the waters in this area. In the Carnegie data, the *T–S* curves divided the areas into two groups, one which almost corresponds to our northern region and the other to our central and southern. Using the Carnegie data, division into such regions appeared to obscure the characteristic pictures of *T–S* curves which indicate the presence of a maximum and minimum at 200 m and 500 m, respectively, found just in the boundary area between these two groups, at about 8°–12° N.

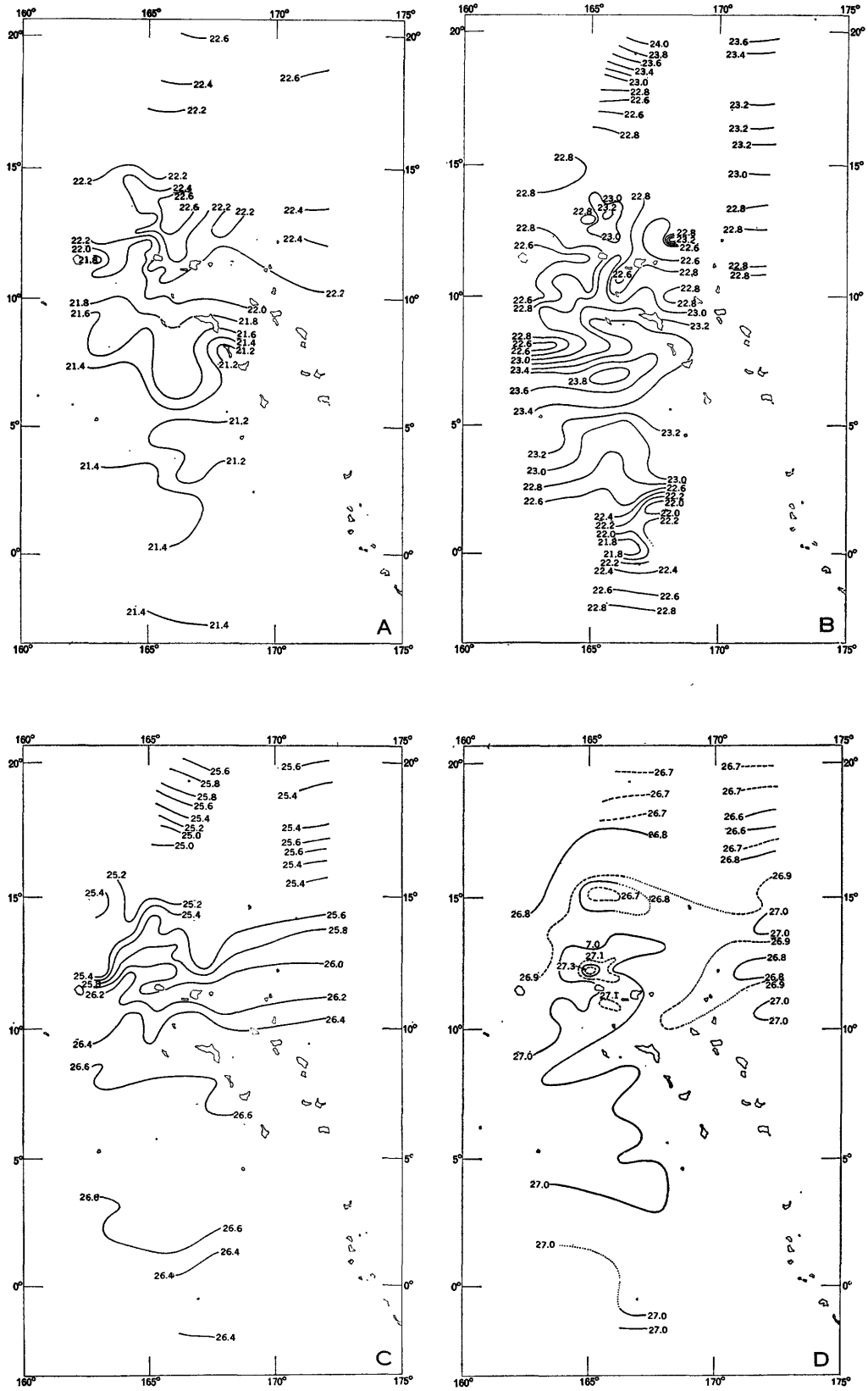

FIGURE 205.—Horizontal distribution of density, from Crossroads data, March to August 1946. *A*, At surface. *B*, At 100 meters. *C*, At 250 meters. *D*, At 500 meters.

IN THE SOUTHERN REGION

[figs. 206, 207, 208, 209]

As was mentioned above, almost the whole water column in this region (between 200 m and 1,000 m) is covered by Equatorial Pacific Water.

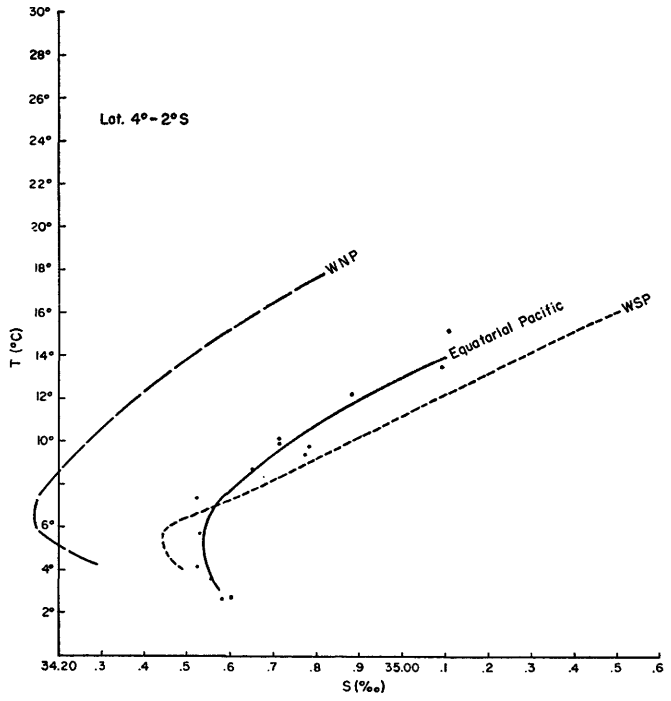

FIGURE 206.—Temperature-salinity (T-S) diagram for 4° S.–2° S., from Crossroads data, March to August 1946.

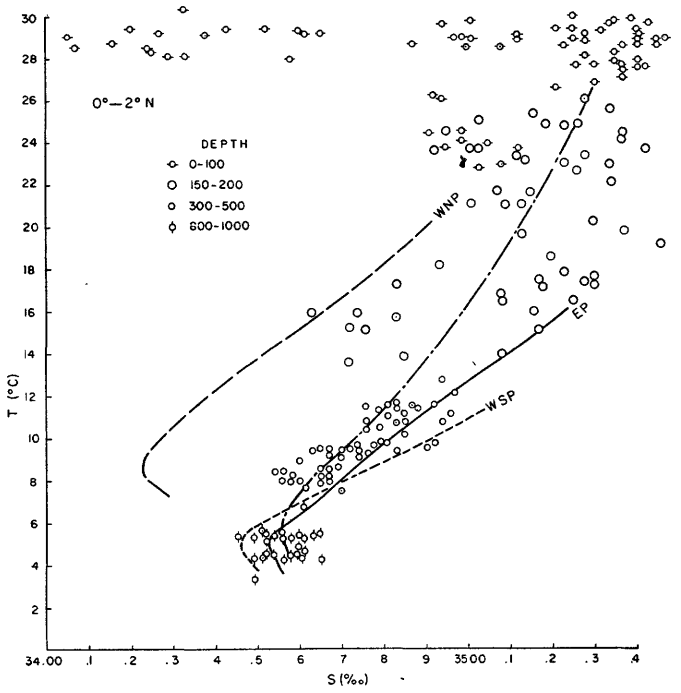

FIGURE 208.—Temperature-salinity (T-S) diagram for 0°–2° N., from Crossroad data, March to August 1946.

In the northern part of this region, at 0°–2° N., some scatter of the values is seen at the 200 m level. However, this scatter does not seem to be of irregular distribution, but indicates that at the 200 m level the transition takes place from Equatorial Pacific Water to Western North Pacific Water, more and more of the

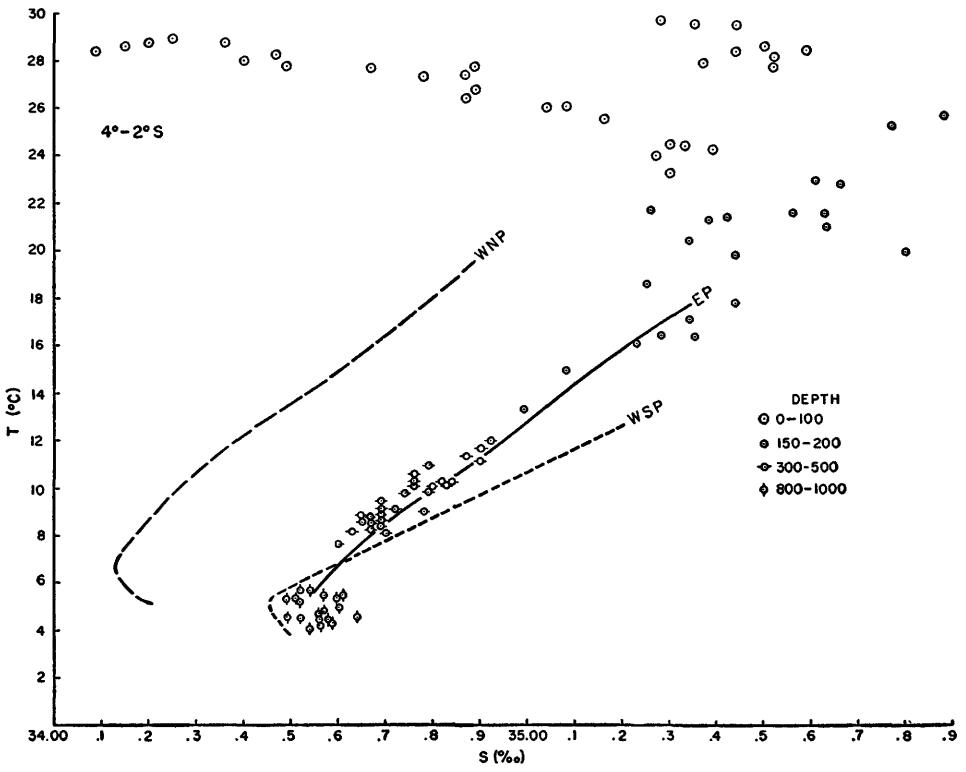

FIGURE 207.—Temperature-salinity (T-S) diagram for 4° S.–2° S., from Japanese data, summer season, 1933–41.

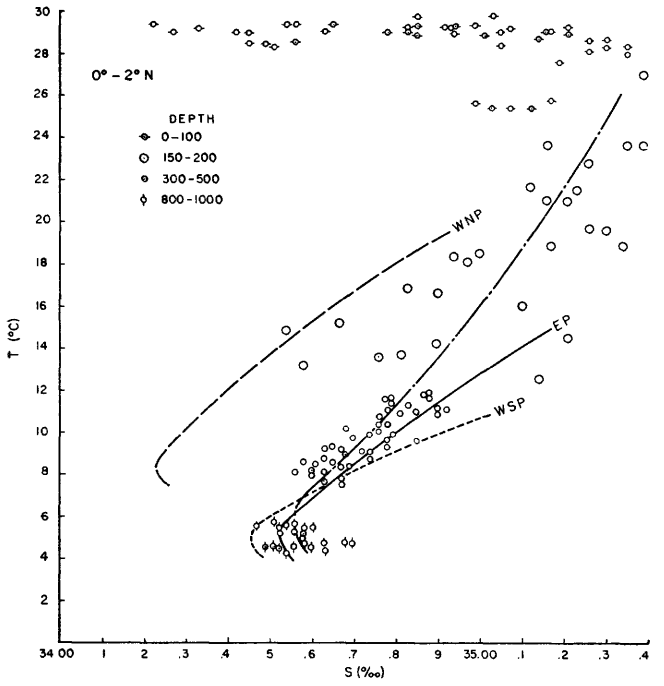

FIGURE 209.—Temperature-salinity (T-S) diagram for 0°–2° N., from Japanese data, winter season, 1933–41.

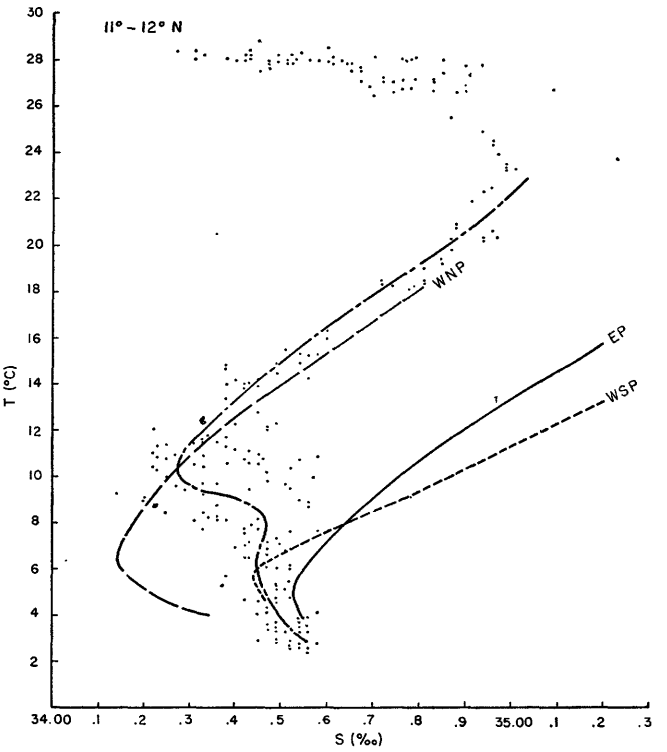

FIGURE 210.—Temperature-salinity (T-S) diagram for 11° N.–12° N., from Cross roads data, March to August, 1946.

latter becoming mixed with Equatorial Pacific Water as the latitude increases until Western North Pacific Water completely replaces Equatorial Pacific Water at about latitude 10° N. It is found from the original data that at 0°–2° N. some of those points which are close to Western North Pacific Water belong to those near 2° N.

IN THE CENTRAL REGION

[figs. 210, 211, 212]

Whereas the Equatorial Pacific Water covers the whole column in the southern region, the typical characteristic in the central region is that Equatorial Pacific Water underlies Western North Pacific Water which covers the upper part of the water column. As was mentioned before, an Intermediate Water of northern origin becomes obscure at the southern part of this region. For this reason, the presence of double maxima and minima is most distinct in the northern part of the region. (See figs. 210, 211, 212).

Below a depth of salinity maximum (100–150 m), Western North Pacific Water exists as a comparatively thin layer, a thickness of about 50 m to 100 m, and below the 300 m level (lower than 6° N.) to the 500 m level (higher than 10° N.), Equatorial Pacific Water exists. The transitional layer has a thickness of about 100 m to 300 m here and Equatorial Pacific Water extends more widely. Thus, besides the upper salinity

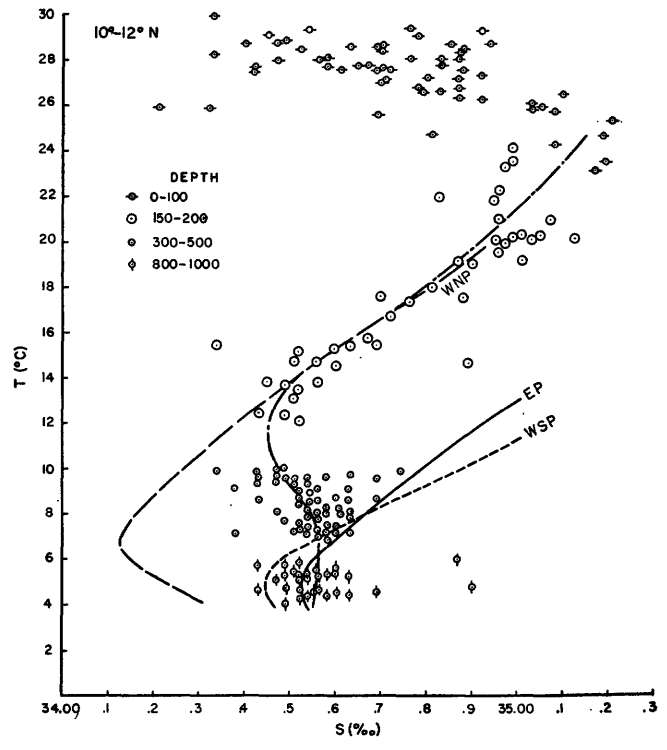

FIGURE 211.—Temperature-salinity (T-S) diagram for 10° N.–12° N., from Japanese data, 1933–41, summer season.

maximum of 150 m there are another salinity maximum and one or two salinity minima. Typical stratification of those water masses is illustrated in figure 213.

Generally in this region, the water of the 200 m level is a transition between Western North Pacific Water and Equatorial Pacific Water. In the northernmost part, at about 10°–12° N., this transitional layer is replaced by 300 m to 400 m layers.

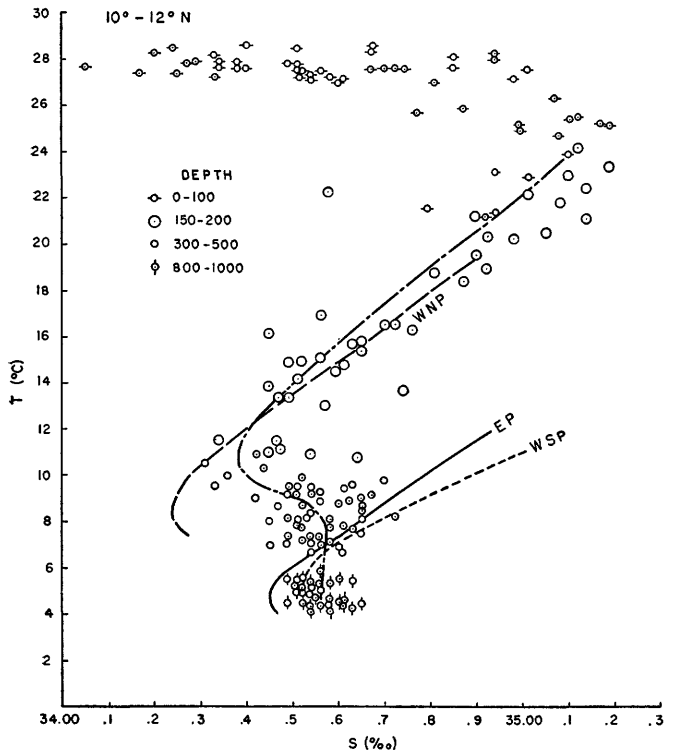

FIGURE 212.—Temperature-salinity (T-S) diagram for 10° N.–12° N., from Japanese data, 1933–41, winter season.

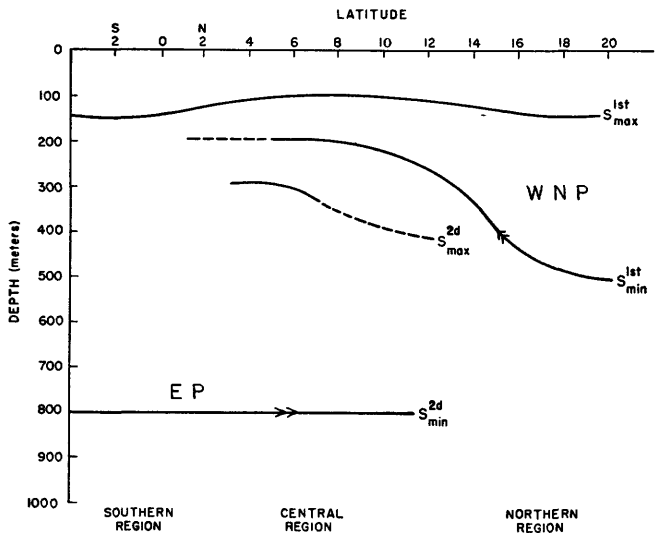

FIGURE 213.—Stratification of water masses in the Marshall Islands area.

IN THE NORTHERN REGION

[figs. 214, 215, 216]

The water in this region is essentially characterized by Western North Pacific Water which covers almost all depths. The thermocline layer is not well defined. A

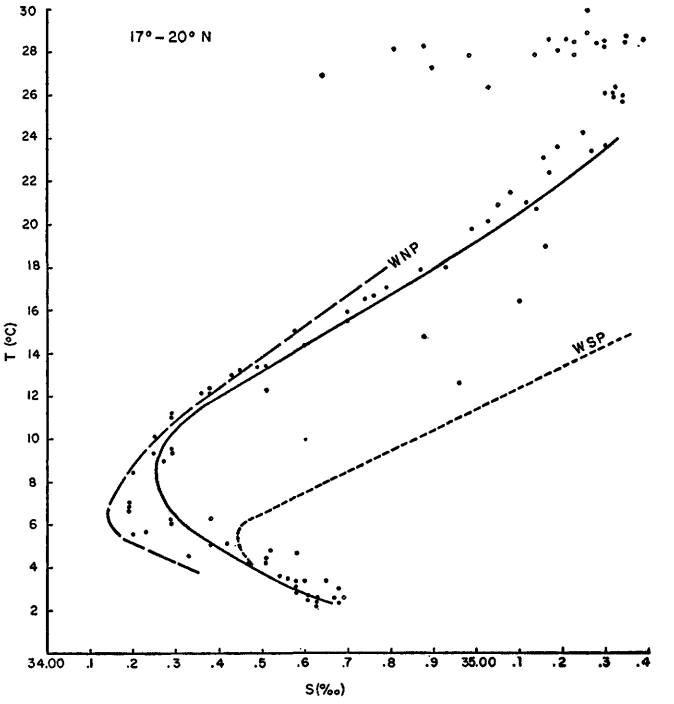

FIGURE 214.—Temperature-salinity (T-S) diagram for 17° N.–20° N., from Crossroads data, March to August 1946.

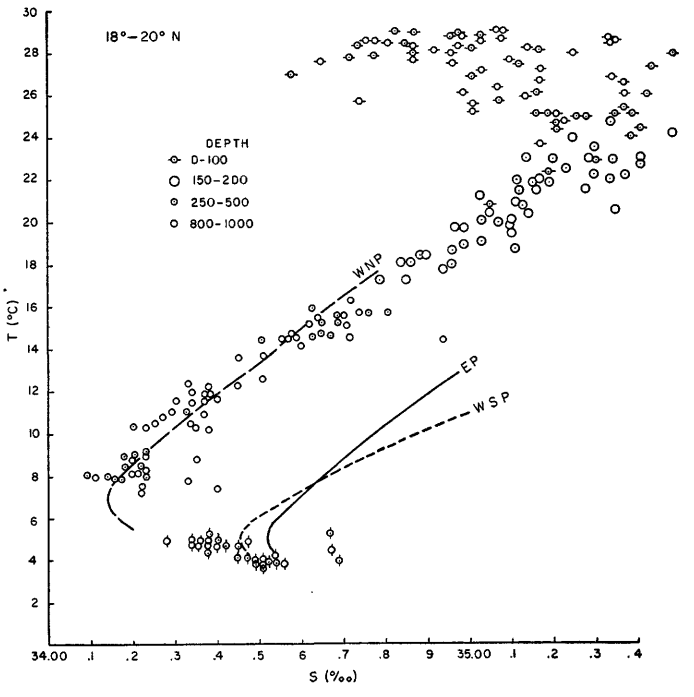

FIGURE 215.—Temperature-salinity (T-S) diagram for 18° N.–20° N., from Japanese data, 1933–41, summer season.

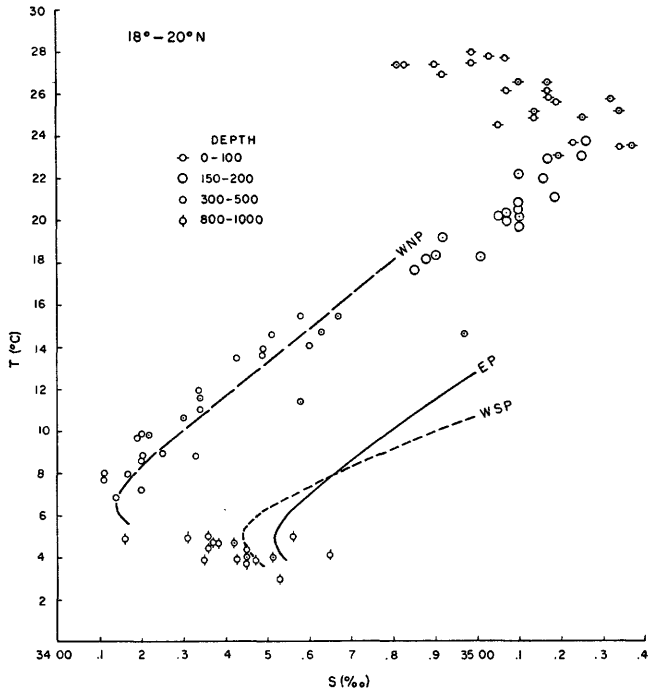

FIGURE 216.—Temperature-salinity (T-S) diagram for 18° N.–20° N., from Japanese data, 1933–41, winter season.

salinity minimum is found at the 500 m level in the T–S diagrams for this region and becomes shallower with decreasing latitude. This layer of salinity minimum is considered to be associated with the core of the Intermediate Water of northern origin, and it continuously ascends to 200 m level in the central region.

It has been mentioned in previous sections that the decrease of depth of salinity-minimum level with decreasing latitude is due to a slow ascending motion of the Intermediate Water of northern origin. The salinity minimum found at a depth of 200 m to 500 m is considered of this nature. The fact that this minimum level becomes less and less distinct towards the Equator lower than 8° N. is a good indication of the southward travel of this water.

These investigations appear to indicate that another Intermediate Water travels northward at deeper levels from the south. The second minimum of salinity found at about 800 m in low latitudes may correspond to the center of the Intermediate Water of southern origin.

Temperature at the first salinity-minimum level decreases with latitude from 15° C at latitude 2°–4° N to 7° C at latitude 18°–20° N. The corresponding values of salinity and σ_t are from 34.70°/₀₀ to 34.20°/₀₀ and from 26.2 to 26.7. Since it appears that the Intermediate Water of the northern origin is characterized by σ_t=26.7, T=6.5° C, and S=34.0°/₀₀ in the source of the origin (Koenuma, 1939), the above may indicate the ascending southward travel of this Intermediate Water. It is seen that in the northern region the identity of this Intermediate Water is preserved, while in the central and southern region, this Intermediate Water is greatly mixed with the overlying water. In the second salinity-minimum level, values of T, S, and σ_t in our area remain almost constant—T=5.5°, S=34.55°/₀₀, and σ_t=27.2. The Intermediate Water of southern origin is characterized by σ_t=27.2–27.4 (Sverdrup and others, 1946, p. 744).

For an easy comprehension of the gradual changes of water masses in this area, the table below shows the respective depths and salinity readings of the first and the second salinity maxima and minima for an interval of every 2 degrees of latitude.

Salinity maxima and minima in the southern, central, and northern regions

[The values in the parentheses are not well defined]

Region	Lat. (°)	Salinity maxima and minima							
		1st maximum		1st minimum		2d maximum		2d minimum	
		Depth (m)	Salinity (°/₀₀)	Depth (m)	Salinity (°/₀₀)	Depth (m)	Salinity (°/₀₀)	Depth (m)	Salinity (°/₀₀)
Southern	4S	150	35.5	----	----	----	----	800	34.55
	2S	150	35.5	----	----	----	----	800	34.55
	0	125	35.3	(200)	(34.6)	----	----	800	34.55
Central	2N	125	35.2	(200)	(34.6)	300	34.72	800	34.55
	4N	125	35.0	200	34.55	300	34.65	800	34.55
	6N	125	34.9	200	34.55	350	34.65	800	34.55
	8N	100	34.9	200	34.45	(400)	34.65	800	34.55
	10N	125	35.0	250	34.4	(400)	34.58	800	----
	12N	125	35.1	300	34.4	----	----	----	----
Northern	14N	130	35.2	400	34.4	----	----	----	----
	16N	140	35.25	500	34.25	----	----	----	----
	18N	140	35.25	500	34.2	----	----	----	----
	20N								

REMARKS ON THE DISTRIBUTION OF OXYGEN

Only a few remarks on the characteristic features of oxygen distribution can be made here, because the number of oxygen data available for the Marshall Islands area is small and because very little is known about the consumption of oxygen through biological activities in this area. Attention is directed to the two vertical sections of oxygen distribution (fig. 217) from the Crossroads and the Japanese data for the summer season, respectively. Winter data are not detailed enough to plot a reasonable section. Four charts of horizontal distributions of oxygen at the surface, and at the 100 m, 250 m, and 500 m levels from the Crossroads data were prepared as usual. However, since those charts do not add to our knowledge materially, they will not be discussed separately.

The major features of oxygen distribution in the area of concern are:

1. A triple division of the vertical distribution of oxygen in sea water is (1) an oxygen-saturated layer at and near the sea surface, (2) an oxygen-minimum layer at the intermediate depth, and (3) an oxygen-rich layer at the greater depth. (Sweiwell, 1935.) This division is distinctively shown in both sections. At and very near the surface, oxygen concentration is invariably, from both the Crossroads and the Japanese results, around 4.0 ml–4.5 ml/l at all latitudes concerned.

2. In the Japanese section, a subsurface layer (presumably a layer of oxygen supersaturation) of oxygen concentration higher than the surface value clearly appears. This feature is thought to be probably caused by one (or both) of the following:

The intrusion of the northern Tropical Water mass. Favorable evidence for this argument is the exceptional coincidence of the location and the direction of the 4.75 ml/l oxygen-concentration isoline (fig. 217*B*) and the salinity-maximum tongue (fig. 193*B*) which was presumably considered as the axis of the northern Tropical Water mass.

The high production of oxygen by plants in this layer. Favorable arguments in this respect are that (1) a subsurface layer of oxygen supersaturation is quite a common feature in the summer season because of the high production of oxygen by plants and (2) the complete absence of a similar supersaturated layer in the Crossroads section casts some doubt as to the first alternative.

3. The inclinations of isolines of oxygen concentration and the axis of the oxygen-minimum layer (fig. 217*B*) from high latitudes toward the area of large eddies (at about 6°–10° N.) resembles very much the inclination of a salinity-minimum tongue in figure 215. The parallelism of these two features strongly suggests that they are most probably associated with the same phenomenon—that is, the ascending of the Intermediate Water mass from higher to lower latitudes, reaching its shallowest depth at the area of large-size eddies (see sections on salinity distribution and T–S relationship).

4. In the area of large eddies, the distribution of oxygen is characterized by remarkably horizontal isolines of oxygen concentration and exceptionally large vertical gradient. These account for the fact that in horizontal distribution of oxygen in a layer at about 100 m–300 m, oxygen concentration at each relevant depth is phenomenally low (fig. 218*B*, *C*). The main causes of these characteristic features are thought to be:

The high stability at the bottom of the isothermal layer in these latitudes prevents an effective transport of oxygen below the interface of upper mixed layer and underlying layer.

The aged water masses which appear at these latitudes contain less oxygen.

The strong upwelling which occurs there brings up water of low oxygen from some intermediate depth.

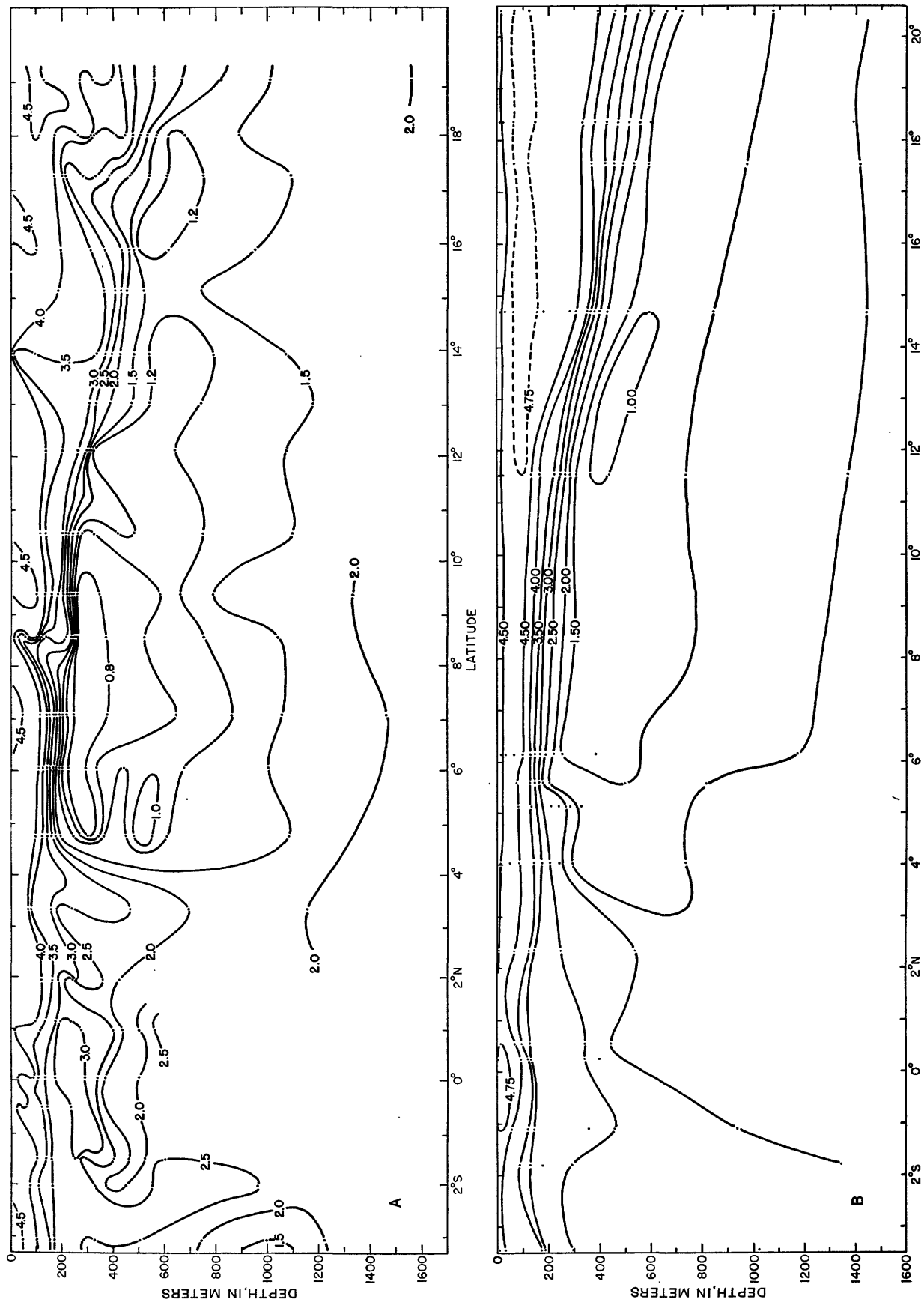

FIGURE 217.—Vertical distribution of oxygen concentration (ml/l). *A*, From Crossroads data, March to August 1946. *B*, From Japanese data, 1933–41, summer season.

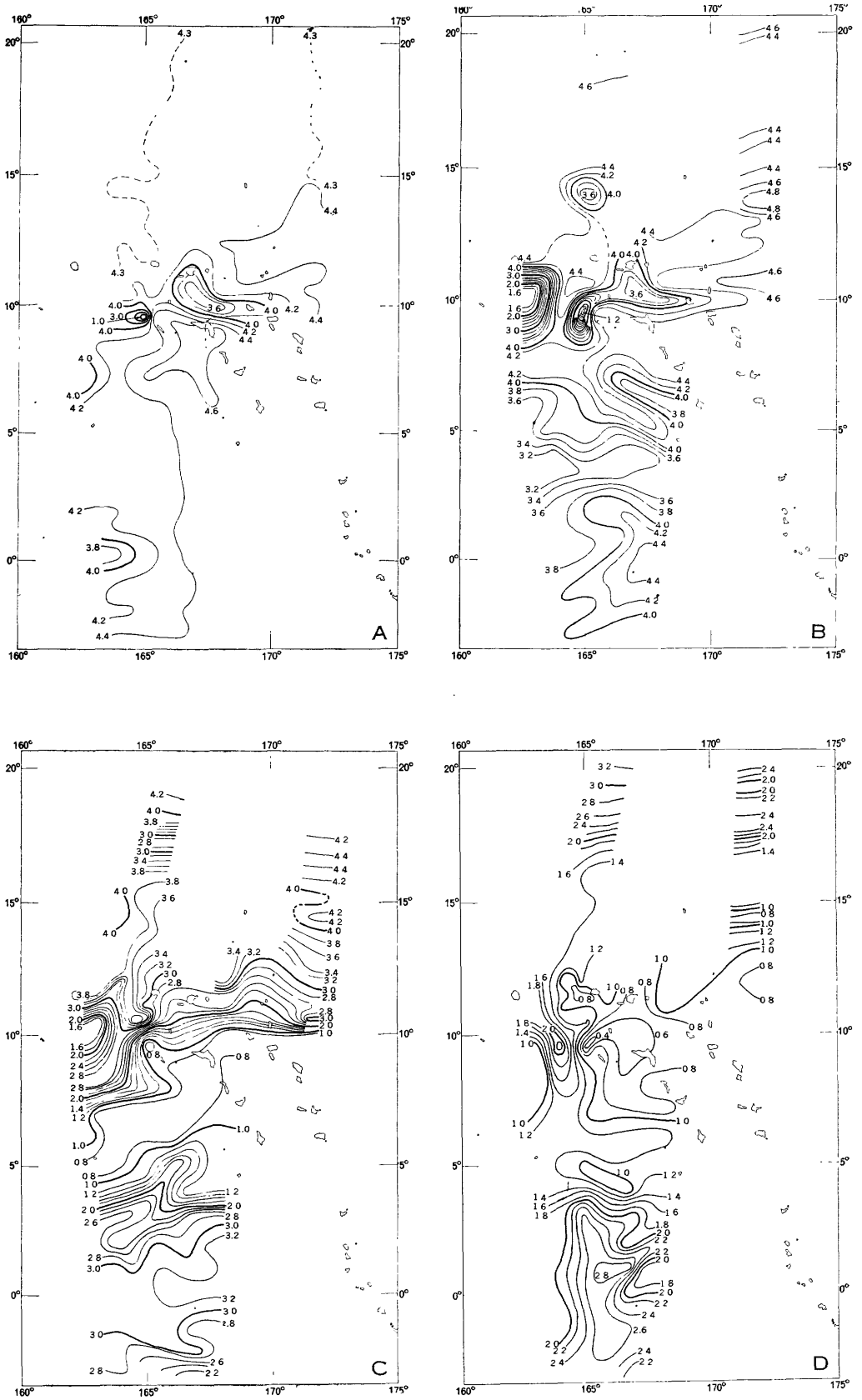

FIGURE 218.—Horizontal distribution of oxygen concentration (ml/l), from Crossroads data, March to August 1946. *A*, At surface. *B*, At 100 meters. *C*, At 250 meters. *D*, At 500 meters.

REFERENCES AND LITERATURE CITED

Barnes, C. A., Bumpus, D. R., and Lyman, John, 1948, Ocean circulation in the Marshall Islands area: Amer. Geophys. Union, Trans., v. 29, p. 871–876.

Cromwell, Townsend, 1950, Mid-Pacific oceanography, January-March 1950: U. S. Department of the Interior, Fish and Wildlife Service, Special Scientific Report Fisheries 54.

Defant, Albert, 1936, Schichtung und Zirkulation der Atlantischen Ozeans: Die Troposphäre. Wiss. Ergebn. deut. Atlant. Meteor., Band 6, Lief. 3, p. 316–326.

Haurwitz, Bernhard, and Panofsky, H. A., 1950, Stability and meandering of the Gulf Stream: Amer. Geophys. Union, Trans., v. 31, p. 723–731.

Jacobs, W. C., 1951, The energy exchange between sea and atmosphere and some of its consequences: Scripps Inst. Oceanography, Bull., 6, p. 27–122.

Japanese Hydrographic Department, 1933, Bulletin of the Hydrographic Department of the Imperial Japanese Navy, v. 6, p. 187–211.

Japanese Hydrographic Bureau, 1948, The Oceanographic Bulletin No. 3.

Japanese Maritime Safety Agency, 1950, The Hydrographic Bulletin, Special Number 3.

——— 1951, The Hydrographic Bulletin, Special Number, 8.

Koenuma, Kwanji, 1939, On the hydrography of the southwestern part of the north Pacific and the Kuroshio, Part III: Imper. Mar. Observ., Memoirs, Japan, v. 7, p. 41–114.

Munk, W. H., 1950, On the wind-driven oceanic circulation: Jour. Meteorology, v. 7, p. 79–93.

Reid, R. O., 1948a, The equatorial currents of the eastern Pacific as maintained by the stress of the wind: Jour. Marine Research, v. 7, p. 74–99.

Reid, R. O., 1948b, A model of the vertical structure of mass in equatorial wind drift currents of a baroclinic ocean: Jour. Marine Research, v. 7, p. 304–312.

Robinson, M. K., 1954, Sea temperature in the Marshall Islands area: U. S. Geol. Survey Professional Paper 260–D, p. 281–292.

Sweiwell, H. R. 1935, The distribution of oxygen in the western basin of the North Atlantic; Papers in Phys. Oceanography and meteorology, v. 3, no. 1.

Sverdrup, H. U. 1947, Wind-driven currents in a baroclinic ocean: with application to the equatorial currents of the eastern Pacific. Nat. Acad. Sci. Proc., v. 33, p. 318–326.

Sverdrup, H. U., and Fleming, J. A., 1944, Scientific results of cruise VII of the CARNEGIE, 1928–29. Oceanography I–A. Observations and results in physical oceanography: Carnegie Inst. Pubs. p. 111.

Sverdrup, H. U., Johnson, M. W., and Fleming, R. R., 1946, The oceans, 2d ed., Prentice-Hall Inc. New York. 1,087 pp.

Uda, Michitaka, 1940, On the recent anomalous hydrographical conditions of the Kuroshio in the south waters off Japan proper in relation to the fisheries: Imper. Fisher. Exper. Sta., Jour., Japan, no. 10, p. 231–278.

——— 1949, On the correlated fluctuations of the Kuroshio and the cold water mass: Oceanog. Mag., Japan, v. 1, p. 1–12.

——— 1952, On the hydrographic fluctuation in the Japan Sea. Preliminary report: 3d anniversary of the Japan Sea Fisheries Research Institute, Memo. p. 291–300.

Yoshida, Kozo, Mao, Han-Lee, and Horrer, Paul L., 1953, Circulation in the upper mixed layer of the equatorial north Pacific: Jour. Marine Research, v. 12, p. 99–120.

○